Hamiltonian theory of the strongly coupled limit of the Kondo problem in the overscreened case

2004 J. Phys.: Condens. Matter 16 6075

(http://iopscience.iop.org/0953-8984/16/34/008)

INSTITUTE OF PHYSICS PUBLISHING JOURNAL OF PHYSICS: CONDENSED MATTER

J. Phys.: Condens. Matter **16** (2004) 6075–6098 PII: S0953-8984(04)79423-0

Hamiltonian theory of the strongly coupled limit of the Kondo problem in the overscreened case

Domenico Giuliano[1,2] **and Arturo Tagliacozzo**[3,4]

[1] Dipartimento di Fisica, Università della Calabria, Italy
[2] INFN, Gruppo collegato di Cosenza, Arcavacata di Rende (CS), I-87036, Italy
[3] Coherentia—(INFM), Unità di Napoli, Napoli, Italy
[4] Dipartimento di Scienze Fisiche Università di Napoli 'Federico II', Monte S. Angelo—via Cintia, I-80126 Napoli, Italy

Received 16 April 2004
Published 13 August 2004
Online at stacks.iop.org/JPhysCM/16/6075
doi:10.1088/0953-8984/16/34/008

Abstract

By properly generalizing Nozières' Fermi liquid theory, we construct a Hamiltonian approach to the scattering of conduction electrons off a spin-1/2 impurity in the overscreened Kondo regime as $T \to 0$. We derive the S-matrix at the interacting fixed point, and the corresponding phase shifts, together with leading energy corrections to the unitary limit. We apply our results to obtain the low-temperature dependence of the two-channel Kondo conductance, and we relate it to possible transport experiments in a quantum dot.

1. Introduction

The Kondo effect in metals containing magnetic impurities consists of an 'anomalous' minimum in the resistivity $\rho(T)$, as the temperature T drops below the 'Kondo temperature' T_K. The minimum is due to antiferromagnetic scattering of conduction electrons off the localized magnetic impurities [1]. Quite recently [2, 3], the signature of Kondo interaction has been found in transport experiments across a quantum dot (CD) at a Coulomb blockade (CB). At CB, the QD is expected to be insulating, due to the discreteness of its levels [3]. Nevertheless, within a CB valley, the linear DC conductance may saturate at low temperatures. As $T > T_K$, the conductance exhibits the typical logarithmic raise [4]. When T drops below T_K, it saturates to its unitary limit, $G = 2e^2/h$. Below T_K, a perturbative approach in the coupling is not feasible.

The single impurity Kondo effect is classified according to the spin s of the impurity and to the number of channels κ of itinerant electrons involved in the scattering. Indeed, electrons scattering off the impurity may be labelled by quantum numbers other than the spin (for instance, angular momentum) [5]. In spite of the fact that in the perturbative temperature region there are no qualitative differences between the one-channel and many-channel effect [6], because of the different nature of the corresponding ground states (GS), deep differences arise in the unitary limit, depending on κ and s. In particular:

- If $\kappa = 2s$, as T is lowered down to 0, the flow of the coupling strength between the impurity magnetic moment and the spin of itinerant electrons runs all the way towards an infinite-coupling fixed point. At the fixed point, the impurity spin is fully screened, and the localized magnetic moment effectively disappears. The impurity rather works as a spinless scattering centre in the Fermi sea of the itinerant electrons, and double occupancy at the impurity site is forbidden ('Noziéres picture' [7]). This is the most common case: a QD with an odd number of electrons behaves as a spin-$1/2$ impurity, interacting with one channel of conduction electrons from the Fermi sea of the contacts.
- If $\kappa < 2s$, the system is 'underscreened'. A residual magnetic moment survives on the impurity, even at $T = 0$. This moment interacts ferromagnetically with the spins of the itinerant electrons. $T = 0$ is again an attractive infinite-coupling fixed point and, accordingly, the system is described by Fermi liquid (FL) theory. An example of this case occurs in a two-dimensional QD in a magnetic field at a singlet–triplet level crossing [8–10].
- If $\kappa > 2s$ and the exchange coupling is the same for both channels, the impurity magnetic moment gets 'overscreened'. An effective residual magnetic moment survives on the impurity, antiferromagnetically interacting with the spin of itinerant electrons. As a consequence, the infinite-coupling fixed point is now repulsive, as well as the non-interacting fixed point. The system flows toward an intermediate, finite-coupling fixed point, where FL theory has been predicted to break down [11].
  The prototype model for this case is the two-channel spin $1/2$ Kondo (2CK) model, whose low-temperature behaviour will be the subject of this paper. Our approach extends the Nozières' picture of the one channel Kondo fixed point [7] to the 2CK case. This allows us to highlight the non-Fermi liquid (NFL) properties within a scattering matrix (S-matrix) approach, which is particularly suitable to studying the conductance across a QD.

The overscreened Kondo effect has been hypothesized to be the driving mechanism of low-energy physics of several systems, although, depending on the physical system involved, the relevant degree of freedom of the impurity may not be its spin, but some orbital angular momentum labelling its energy levels ('orbital Kondo') [12].

For instance, the overscreened Kondo effect has been predicted to possibly take place in glassy metals [13]. Whether it really arises in these systems or not is still a debated question [14]. A two channel Kondo behaviour has been invoked in an experiment by Ralph and Buhrman on clean Cu point contacts [15]. A different route toward the realization of the two-channel Kondo effect in a controlled way has been recently proposed in vertical QDs at a Coulomb blockade [16], or in similar mesoscopic devices [17, 18]. According to the predictions concerning single impurity Kondo models, as $T < T_{\mathrm{K}}$, the temperature dependent corrections to the conductance should display a crossover from log-like dependence on T to a dependence on $(T/T_{\mathrm{K}})^2$ for the perfectly screened case, and on $\sqrt{T/T_{\mathrm{K}}}$ for the overscreened case. In fact, the crossover to a T^2-dependence has been experimentally seen in a vertical QD with few electrons [4]. No experimental evidence for 2CK in dots has been produced yet.

On the theoretical side, due to its connections to many condensed matter problems, the 2CK model has been studied with a number of different techniques [19]. Finite-T corrections have been derived by means, for instance, of Bethe-ansatz like exact solutions [20]. Ludwig and Affleck applied conformal field theory (CFT) techniques to determine finite-T corrections to the unitary limit, Wilson ratios and several exact results concerning Green functions [11]. Numerical renormalization group (RG) techniques applied to multichannel Kondo models have a long history [21–24]. Abelian bosonization [25] and subsequent refermionization [26] has

been used as well as Majorana fermions [27] to study the strongly coupled states by removing the unscattered degrees of freedom. Functional integral methods, including the slave boson technique [28] and the Coulomb gas approach, have also been applied to 2CK [29].

A number of approaches have been applied to describe non-equilibrium properties such as nonlinear conductance, mostly in connection with the Anderson impurity model [2]. These range from the numerical renormalization group, to the non-crossing approximation (NCA) [30, 31], perturbative functional integral methods [32] and perturbative renormalization group methods in real time [33].

In this paper we study the 2CK model close to the fixed point, by applying bosonization and refermionization of the quantum particle fields. We consider a spin $1/2$ impurity at $x = 0$, antiferromagnetically coupled to a right (R) and a left (L) one dimensional non-interacting Fermi sea, with an extra index $\alpha = 1, 2$, which labels the two conduction channels. We employ a scattering approach that is appropriate to study the unitary limit of the conductance at $T = 0$. In particular, this will allow us to calculate both fixed point conductance and the leading temperature dependent corrections. By removing the degrees of freedom not interacting with the impurity in the unitary limit, we move the NFL fixed point to infinite coupling. Accordingly, we apply a perturbative strong coupling expansion. We first derive the properties of the GS at the fixed point in the bosonic representation using the lattice version of the model. Next, going back to fermions in the continuum limit, we obtain a fermionic representation for the fixed point S matrix, and get the unitary limit of the conductance, by using the Landauer formula. Finally, we derive finite T corrections to the DC conductance in bosonic coordinates. In the conclusions we propose a connection between this model and a possible realization of the 2CK conductance in a QD [16].

Our representation of the S matrix does not suffer from the 'unitarity paradox', since, following Ludwig and Maldacena, we introduce a 'spin-flavour' quantum number in the bosonic representation [34]. Indeed, in the unitary limit, the spin flavour is the only quantum number that is alleged to change upon scattering of the impurity. However, some care has to be used when describing such a dynamics in fermionic coordinates.

The paper is organized as follows:

In section 2 we introduce the Hamiltonian with linearized bands close to the Fermi points and the bosonic representation of the relevant quantum fields. Because of the redundancy, due to the spin-flavour field, we define two different bosonic representations for the same fermionic field, which we refer to as I and II.

In section 3 we construct the fixed point impurity GS by reformulating in bosonic coordinates the regularization scheme proposed in [27].

In section 4 we go back to the fermionic representation. Once we have identified the physical states, we implement Nozières' scheme, by deriving a one-body potential for the fixed point fermionic Hamiltonian. This rephrases in fermionic coordinates the spin-flavour bosonic field dynamics due to the scattering off the impurity. Next, we use the Hamiltonian we derive, to calculate the Green functions at the fixed point. The one-particle Green functions provide us with the S matrix elements in the I, II representation. Our approach gives the correct result for the phase shift for each fermion field, given by $\pm\pi/4$.

In sections 5 and 6 we employ a Schrieffer–Wolff-like transformation to derive the corrections to the fixed point Hamiltonian. In particular, in section 5 we show that the first correction, although irrelevant for what concerns the fixed point dynamics, selects the appropriate physical states at any point. The unitary limit for the conductance follows immediately, provided the degrees of freedom are properly counted. In section 6 we derive the first irrelevant operator, giving an energy dependent correction to the phase shifts in the S-matrix and, consequently, a T-dependent correction to the conductance.

In section 7 we summarize our conclusions and relate our results to the existing experimental quest for 2CK in QDs.

Mathematical details of the derivation are reported in appendices A–D.

2. The two-channel Kondo Hamiltonian: low-energy fermion modes and bosonization

In this section we introduce the model Hamiltonian for lead electrons in the overscreened Kondo effect. Since in the following we will need the lattice version of the Hamiltonian, we start by introducing the lattice version of the theory. We will propose the fermionic and the bosonic version of the model Hamiltonian.

On a system of size L, the lattice kinetic energy in Fourier space is given by:

$$H_{\rm T} = \sum_{k_\ell;\sigma\alpha} [\mu - 4t\cos(k_\ell a)] c^\dagger_{\sigma\alpha}(k_\ell) c_{\sigma\alpha}(k_\ell) \tag{1}$$

(the cs are fermionic operators in momentum space, $k_\ell = 2\pi\ell/L$; $\ell = 0\cdots N-1$, μ is the chemical potential, a is the lattice step, α is the channel index).

In the long wavelength limit, expanding about the two Fermi points, one gets the effective Hamiltonian:

$$H_{\rm T} = -{\rm i}v_f \int {\rm d}x \sum_{\sigma\alpha} \left\{ \phi^\dagger_{R;\sigma\alpha}(x) \frac{\rm d}{{\rm d}x} \phi_{R;\sigma\alpha}(x) - \phi^\dagger_{L;\sigma\alpha}(x) \frac{\rm d}{{\rm d}x} \phi_{L;\sigma\alpha}(x) \right\}, \tag{2}$$

where $v_f = 4ta\sin(ak^+_{\rm F})/2\pi$, and:

$$\phi_{L/R,\sigma\alpha}(x) = \int {\rm d}p\, {\rm e}^{{\rm i}px} \phi_{L/R,\sigma\alpha}(p). \tag{3}$$

The isotropic lattice Kondo interaction Hamiltonian is given by:

$$H^{\rm 2CK}_{\rm K} = J\mathbf{S}_d \cdot [\vec{\sigma}_1(0) + \vec{\sigma}_2(0)], \tag{4}$$

where $\vec{\sigma}_\alpha(x) = \frac{1}{2}\sum_{\sigma\sigma',\alpha} c^\dagger_{\sigma\alpha}(x)\vec{\tau}_{\sigma\sigma'}c_{\sigma'\alpha}(x)$ and $\mathbf{S}_d$ is the spin 1/2 impurity located at $x = 0$.

By using the linear combinations:

$$\begin{aligned} \phi_{{\rm e};\sigma\alpha}(x) &= \frac{1}{\sqrt{2}}[\phi_{R;\sigma\alpha}(x) + \phi_{L;\sigma\alpha}(-x)] \\ \phi_{{\rm o};\sigma\alpha}(x) &= \frac{1}{\sqrt{2}}[\phi_{R;\sigma\alpha}(x) - \phi_{L;\sigma\alpha}(-x)], \end{aligned} \tag{5}$$

$H^{\rm 2CK}_{\rm K}$ takes the form:

$$H^{\rm 2CK}_{\rm K} = J\mathbf{S}_d \cdot [\vec{\sigma}_{{\rm e};1}(0) + \vec{\sigma}_{{\rm e};2}(0)], \tag{6}$$

where

$$\vec{\sigma}_{{\rm e};\alpha}(x) = \tfrac{1}{2}\sum_{\sigma\sigma'} \phi^\dagger_{{\rm e};\sigma\alpha}(x)\vec{\tau}_{\sigma\sigma'}\phi_{{\rm e};\sigma'\alpha}(x),$$

that is, only the 'e'-fields enter the Kondo interaction Hamiltonian. As a consequence, we may study the Kondo dynamics by taking into account only the chiral fields $\phi_{{\rm e};\sigma\alpha}$. From now on, we will drop the suffix e from the various field operators.

In order to properly deal with the interacting fields, we bosonize $\phi_{\sigma\alpha}$ [11]. Since we have four independent fermionic fields, we need the same number of independent bosonic fields, $\Psi_{\sigma\alpha}$. Therefore, following [34], we define:

$$\phi_{\sigma\alpha}(x) = \eta_{\sigma\alpha} {:}{\rm e}^{-{\rm i}\Psi_{\sigma\alpha}(x)}{:}, \tag{7}$$

where $\eta_{\sigma\alpha}$ are real Klein factors, obeying the anticommutator algebra $\{\eta_{\sigma\alpha}, \eta_{\tau\beta}\} = \delta_{\sigma\tau}\delta_{\alpha\beta}$.

It is possible to introduce the densities of physical quantities starting from the linear combinations [34, 26]:

$$\Psi_{\rm ch}(x) = \sum_{\alpha\sigma} \Psi_{\alpha\sigma}(x); \qquad \Psi_{\rm sp}(x) = \sum_{\alpha\sigma} \sigma \Psi_{\alpha\sigma}(x); \qquad \Psi_{\rm fl}(x) = \sum_{\alpha\sigma} \alpha \Psi_{\alpha\sigma}(x). \tag{8}$$

(In equation (8) and in the following, whenever we use σ and α as coefficients we mean $+, -1$, when $\sigma = \uparrow, \downarrow$, and $+, -1$, when $\alpha = 1, 2$.)

The densities of charge, spin and flavour, $\rho_{\rm ch}$, $\rho_{\rm sp}$, $\rho_{\rm fl}$, are given by:

$$\rho_{\rm ch/sp/fl}(x) = \frac{1}{2\pi}\frac{\mathrm{d}}{\mathrm{d}x}\Psi_{\rm ch/sp/fl}(x).$$

Out of the fields $\Psi_{\alpha\sigma}$, a fourth bosonic field, the 'spin-flavour' field, independent of the first three ones, may be constructed, given by:

$$\Psi_{\rm sf}(x) = \sum_{\alpha\sigma} \sigma\alpha \Psi_{\alpha\sigma}(x). \tag{9}$$

The free dynamics of the bosonic fields Ψ is given by the bosonized version of equation (2), that is:

$$H_{\rm Bos} = \frac{v_f}{4\pi}\int \mathrm{d}x \sum_{X={\rm ch,sp,fl,sf}} \left(\frac{\mathrm{d}\Psi_X}{\mathrm{d}x}\right)^2. \tag{10}$$

Notice that the spin-flavour quantum number appears to be 'redundant', as the state of the lead electrons is fully determined by charge, spin and flavour. Indeed, it is possible to realize two 'inequivalent' representations of the fields $\phi_{\sigma\alpha}$ in terms of the four fields Ψ_X ($X =$ ch, sp, fl, sf). The former representation, which we will refer to as $\phi^{\rm I}_{\sigma\alpha}$, is given by:

$$\phi^{\rm I}_{\sigma\alpha}(x) = \eta_{\sigma\alpha}{:}\mathrm{e}^{-\frac{\mathrm{i}}{2}[\Psi_{\rm ch}(x)+\sigma\Psi_{\rm sp}(x)+\alpha\Psi_{\rm fl}(x)+\alpha\sigma\Psi_{\rm sf}(x)]}{:}. \tag{11}$$

The latter representation, instead, is defined by:

$$\phi^{\rm II}_{\sigma\alpha}(x) = \xi_{\sigma\alpha}{:}\mathrm{e}^{-\frac{\mathrm{i}}{2}[\Psi_{\rm ch}(x)+\sigma\Psi_{\rm sp}(x)+\alpha\Psi_{\rm fl}(x)-\alpha\sigma\Psi_{\rm sf}(x)]}{:}. \tag{12}$$

The 'Klein-like' factors $\xi_{\sigma\alpha}$ are determined by the requirement that the fields in the two representations anticommute with each other. Such a requirement is achieved upon defining:

$$\xi_{\sigma\alpha} \equiv \mathrm{e}^{-\mathrm{i}\frac{\pi}{2}\tilde{N}_{\sigma\alpha}}\eta_{\sigma\alpha},$$

where the operators $\tilde{N}_{\sigma\alpha}$ are given by:

$$\tilde{N}_{\sigma\alpha} = \int \mathrm{d}x\,[\rho_{\rm ch}(x) + \sigma\rho_{\rm sp}(x) + \alpha\rho_{\rm fl}(x) - \alpha\sigma\rho_{\rm sf}(x)]$$

(notice the unusual definition of ξ, which involves non-real fermionic factors. Nevertheless, both I and II representations provide perfectly legitimate fermionic fields).

In appendix A we prove that fields within the same representations obey the usual anticommutation relations, while fields from different representations anticommute with each other, that is:

$$\{\phi^a_{\sigma\alpha}(x), \phi^{b\dagger}_{\tau\beta}(y)\} = \delta^{ab}\delta_{\sigma\tau}\delta_{\alpha\beta}\delta(x-y) \tag{13}$$

($a, b =$ I, II).

We now start the derivation of the effective Hamiltonian in the unitary limit.

3. Fixed point impurity ground state in bosonic coordinates

To derive the effective theory for the spin-1/2 overscreened Kondo system in the unitary limit, we use the regularization scheme introduced in [27]. Such an approach allows for moving the intermediate coupling fixed point towards infinite coupling. In particular, we will reformulate the approach used in [27] in terms of bosonic fields, rather than in terms of Majorana fermionic fields. Our formalism allows for a direct derivation of the subleading, finite temperature/frequency corrections to the fixed-point dynamics.

In bosonic coordinates, the Kondo interaction Hamiltonian is given by:

$$H_{\rm K}^{\rm 2CK} = J\left\{ S_d^+ :{\rm e}^{{\rm i}\Psi_{\rm sp}(0)}: :\cos(\Psi_{\rm sf}(0)): + S_d^- :{\rm e}^{-{\rm i}\Psi_{\rm sp}(0)}: :\cos(\Psi_{\rm sf}(0)): + S_d^z \frac{1}{2\pi}\frac{{\rm d}\Psi_{\rm sf}(0)}{{\rm d}x}\right\}$$
$$\equiv J\mathbf{S}_d \cdot [\vec{\Sigma}_A(0) + \vec{\Sigma}_B(0)], \tag{14}$$

where the spin densities $\vec{\Sigma}_{A/B}(x)$ are given by:

$$\vec{\Sigma}^z_{A/B}(x) = \frac{1}{4\pi}\frac{\rm d}{{\rm d}x}[\Psi_{\rm sp} \pm \Psi_{\rm sf}](x); \qquad \vec{\Sigma}^{\pm}_{A/B}(x) = \frac{1}{\sqrt{2}} :{\rm e}^{\pm {\rm i}[\Psi_{\rm sp}\pm\Psi_{\rm sf}](x)}:. \tag{15}$$

In appendix A we prove that both $\vec{\Sigma}_A(x)$ and $\vec{\Sigma}_B(x)$ are $SU(2)$ spin-1/2 operators, and show that the corresponding spinors at a point x are realized as:

$$|\sigma, A\rangle_x = :{\rm e}^{{\rm i}\frac{\sigma}{2}[\Psi_{\rm sp}+\Psi_{\rm sf}](x)}: |{\rm bvac}\rangle,$$

and

$$|\sigma, B\rangle_x = :{\rm e}^{{\rm i}\frac{\sigma}{2}[\Psi_{\rm sp}-\Psi_{\rm sf}](x)}: |{\rm bvac}\rangle. \tag{16}$$

The doublet $|\sigma, A/B\rangle_x$ provides a spinor representation of the $SU(2)$ group generated by

$$\vec{\Sigma}_{A/B} = \int {\rm d}y\, \vec{\Sigma}_{A/B}(y). \tag{17}$$

Also, we obtain

$$\vec{\Sigma}_A|\sigma, B\rangle_x = \vec{\Sigma}_B|\sigma, A\rangle_x = 0, \tag{18}$$

because

$$[\vec{\Sigma}_A, {\rm e}^{\pm\frac{\rm i}{2}[\Psi_{\rm sp}+\Psi_{\rm sf}](x)}] = [\vec{\Sigma}_B, {\rm e}^{\pm\frac{\rm i}{2}[\Psi_{\rm sp}-\Psi_{\rm sf}](x)}] = 0.$$

Equation (18) states that, if at a point x the spin density associated to $\vec{\Sigma}_A$ is $\neq 0$, then, at the same point, the spin density associated to $\vec{\Sigma}_B$ is $= 0$, and vice versa.

Such a statement is the key argument used in [27] to argue that, within such a regularization scheme, the finite-coupling fixed point is actually moved to an infinite-coupling point. The argument is that, since it is not possible to have at the same point both spin densities different from 0, it is also impossible to produce a more-than-1/2-spin composite at the origin to overscreen the impurity spin. Therefore, the unstable overscreened fixed point disappears and NFL-behaviour is reached at an infinitely strong coupled fixed point, where the impurity spin will be fully screened in a localized spin singlet. Such a singlet must be formed either between $\mathbf{S}_d$ and $\vec{\Sigma}_A(0)$, or between $\mathbf{S}_d$ and $\vec{\Sigma}_B(0)$. Therefore, at the fixed point the system can lie within either one of the two singlets $|{\rm Sin}, A, \{\Xi\}\rangle$, $|{\rm Sin}, B, \{\Xi\}\rangle$, given by:

$$|{\rm Sin}, A, \{\Xi\}\rangle = \left(\frac{2\pi\eta}{L}\right)^{\frac{1}{4}} \frac{1}{\sqrt{2}}\{|\Uparrow\rangle \otimes |\downarrow, A, \{\Xi\}\rangle - |\Downarrow\rangle \otimes |\uparrow, A, \{\Xi\}\rangle\}$$
$$|{\rm Sin}, B, \{\Xi\}\rangle = \left(\frac{2\pi\eta}{L}\right)^{\frac{1}{4}} \frac{1}{\sqrt{2}}\{|\Uparrow\rangle \otimes |\downarrow, B, \{\Xi\}\rangle - |\Downarrow\rangle \otimes |\uparrow, B, \{\Xi\}\rangle\}, \tag{19}$$

where η is the convergence factor (see appendix A for details) and $|\Uparrow\rangle$, $|\Downarrow\rangle$ are the two impurity states with opposite spin polarizations. $|\uparrow, A/B, \{\Xi\}\rangle$, and $|\downarrow, A/B, \{\Xi\}\rangle$ are states of conduction electrons with an $\uparrow$ or a $\downarrow$ A/B particle at $x = 0$, respectively, the state of all the other delocalized particles (globally denoted by $\{\Xi\}$) being unspecified for the time being.

Let us, now, define the operator $\mathcal{Q}_x$:

$$\mathcal{Q}_x = \left(\frac{2\pi\eta}{L}\right)^{\frac{1}{2}} [:\mathrm{e}^{\mathrm{i}\Psi_{\mathrm{sf}}(x)}: + :\mathrm{e}^{-\mathrm{i}\Psi_{\mathrm{sf}}(x)}:]. \tag{20}$$

It is straightforward to verify that $[\mathcal{Q}_x]^2 = 1$, $\forall x$. Therefore, its eigenvalues are ± 1.

Since $[\mathcal{Q}_0, H_{\mathrm{K}}^{2\mathrm{CK}}] = 0$,where $\mathcal{Q}_0 = \mathcal{Q}_{x=0}$ one may build simultaneous eigenstates of the two operators, given by:

$$\begin{aligned} |\mathrm{Sin}, +, \{\Xi\}\rangle &= \frac{1}{\sqrt{2}}[|\mathrm{Sin}, A, \{\Xi\}\rangle + \mathrm{i}|\mathrm{Sin}, B, \{\Xi\}\rangle] \\ |\mathrm{Sin}, -, \{\Xi\}\rangle &= \frac{1}{\sqrt{2}}[|\mathrm{Sin}, A, \{\Xi\}\rangle - \mathrm{i}|\mathrm{Sin}, B, \{\Xi\}\rangle]. \end{aligned} \tag{21}$$

Notice that these states are not eigenstates of the spin-flavour.

The construction will be repeated in the next section, where we switch back to the fermion representation.

4. Fixed point fermionic S-matrix

In this section we reformulate the results of section 3 in fermionic coordinates. We will eventually get to the formula for the appropriate scattering potential in the unitary limit. Finally, we will take the continuum limit of our result, and derive the single-particle S-matrix for scattering of the impurity.

In bosonic coordinates, the two different representations for the lattice fermionic fields $c_{\sigma\alpha}(x)$, which we will refer to as $c_{\sigma\alpha}^{\mathrm{I/II}}(x)$, are given by:

$$c_{\sigma\alpha}^{\dagger,\mathrm{I/II}}(x) = \left(\frac{2\pi\eta}{L}\right)^{\frac{1}{2}} :\mathrm{e}^{\frac{\mathrm{i}}{2}[\Psi_{\mathrm{ch}}(x)+\sigma\Psi_{\mathrm{sp}}(x)+\alpha\Psi_{\mathrm{sf}}(x)\pm\alpha\sigma\Psi_{\mathrm{sf}}(x)]}:. \tag{22}$$

In terms of $c_{\sigma\alpha}^{\mathrm{I/II}}(x)$, one may write down the relevant operators acting on one-particle states: the identity operator at point x

$$\mathbf{1}_x = \sum_{\sigma\alpha} [c_{\sigma\alpha}^{\dagger,\mathrm{I}}(x) c_{\sigma\alpha}^{\mathrm{I}}(x) + c_{\sigma\alpha}^{\dagger,\mathrm{II}}(x) c_{\sigma\alpha}^{\mathrm{II}}(x)], \tag{23}$$

and

$$\mathcal{Q}_x = \mathrm{i} \sum_{\sigma\alpha} (\sigma\alpha) [c_{\sigma\alpha}^{\dagger,\mathrm{I}}(x) c_{\sigma\alpha}^{\mathrm{II}}(x) - c_{\sigma\alpha}^{\dagger,\mathrm{II}}(x) c_{\sigma\alpha}^{\mathrm{I}}(x)]. \tag{24}$$

At a point x, $\mathcal{Q}_x$ swaps representations I and II with each other. Moreover, since in bosonic coordinates, at $x = 0$, $[\mathcal{Q}_0, H_{\mathrm{K}}^{2\mathrm{CK}}] = 0$, we require the same thing to hold in fermionic coordinates.

Following Nozières' approach, we construct an effective fixed point Hamiltonian by introducing an infinite-strength repulsive potential scattering at the origin, and by making it commute with $\mathcal{Q}_0$. Therefore, it is given by:

$$V_{\mathrm{fp}} = \mathcal{P}_0 \left\{ \lim_{\lambda\to\infty} \left[\lambda \sum_{\sigma\alpha;a} c_{\sigma\alpha}^{\dagger a}(0) c_{\sigma\alpha}^{a}(0) \right] \mathcal{P}_0 \right\}, \tag{25}$$

where $\mathcal{P}_0 = \frac{1}{2}[\mathbf{1}_0 + \mathcal{Q}_0]$, and λ is the strength of the interaction.

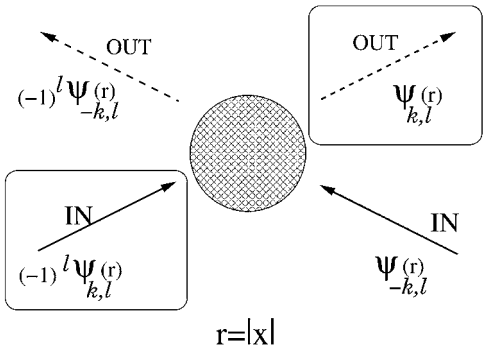

Figure 1. Pictorial sketch of the even–odd decomposition of the scattering process in the (x, t) plane[5]. The heavy dot at the centre is the scattering centre located at $x = 0$. Ingoing and outgoing single particle wavefunctions are shown. One of the chiral components in the scattering has been boxed.

We obtain the unitary Hamiltonian by adding the lattice kinetic energy term to $V_{\rm fp}$. By taking the continuum limit of the corresponding operator, one gets the 'Nozières like' fixed point Hamiltonian. At finite λ, this is given by:

$$H^{\rm 2CK}_{\lambda} \approx \int {\rm d}x \sum_{\sigma\alpha} \{ (\phi^{\dagger,{\rm I}}_{\sigma\alpha}(x) \quad \phi^{\dagger,{\rm II}}_{\sigma\alpha}(x)) \times \left[-{\rm i}v_f \frac{\rm d}{{\rm d}x} \cdot \begin{pmatrix} 1 & 0 \\ 0 & 1 \end{pmatrix} + \lambda\delta(x) \cdot \begin{pmatrix} 1 & -{\rm i}(\sigma\alpha) \\ {\rm i}(\sigma\alpha) & 1 \end{pmatrix} \right] \begin{pmatrix} \phi^{\rm I}_{\sigma\alpha}(x) \\ \phi^{\rm II}_{\sigma\alpha}(x) \end{pmatrix} \Big\}. \tag{26}$$

This Hamiltonian envisages a scattering process for the even component of the field, which is represented pictorially by the boxed field in figure 1.

At $x = 0$ the projected scattering potential exchanges the two representations. Accordingly, $H^{\rm 2CK}_{\lambda}$ is diagonal in the representation index everywhere, except at the origin. In the following, we use $H^{\rm 2CK}_{\lambda}$ to derive the fixed point one-particle Green functions. From the Green functions we derive the fixed point S matrix, which we will eventually use to compute the fixed point conductance.

Let us write down the equations of motion for imaginary time one-particle Green functions, derived from the chiral Hamiltonian of equation (26). For simplicity, here we just consider $\sigma = \uparrow$ and $\alpha = 1$. The Green functions are defined as ($a, b = {\rm I}, {\rm II}$):

$$G^{a,b}_{\uparrow 1}(x, \tau; x', \tau') = \theta(\tau - \tau') \, {\rm Tr} \left[\frac{{\rm e}^{-\beta H}}{\mathcal{Z}} \phi^{a}_{\uparrow 1}(x, \tau) \phi^{\dagger,b}_{\uparrow 1}(x', \tau') \right] - \theta(\tau' - \tau) {\rm Tr} \left[\frac{{\rm e}^{-\beta H}}{\mathcal{Z}} \phi^{\dagger,b}_{\uparrow 1}(x', \tau') \phi^{a}_{\uparrow 1}(x, \tau) \right], \tag{27}$$

where $\beta = 1/k_{\rm B}T$ and $\mathcal{Z}$ is the partition function.

[5] For a one-dimensional elastic channel with momentum k, the scattering amplitudes f are defined by

$$\Psi_k(x) = \begin{cases} {\rm e}^{{\rm i}kx} + f_> {\rm e}^{{\rm i}kx} & x \gg 0 \\ {\rm e}^{{\rm i}kx} + f_< {\rm e}^{-{\rm i}kx} & x \ll 0. \end{cases}$$

The even and odd parity components ($l = {\rm e}$ and $l = {\rm o}$), together with the corresponding amplitudes, are defined by:

$$\Psi_k(x) = [\cos(kr) + f_{\rm e}{\rm e}^{{\rm i}kr}] + {\rm sgn}(x)[{\rm i}\sin(kr) + f_{\rm o}{\rm e}^{{\rm i}kr}] \equiv \psi_{k,{\rm e}}(r) + {\rm sgn}(x)\psi_{k,{\rm o}}(r),$$

where $r \equiv |x|$ and $f_{\rm e} = \frac{1}{2}(f_< + f_>)$ and $f_{\rm o} = \frac{1}{2}(f_> - f_<)$.

The coupled equations of motion for $G^{\mathrm{I,I}}_{\uparrow 1}$ and $G^{\mathrm{II,I}}_{\uparrow 1}$ read:

$$\left(\frac{\partial}{\partial\tau}+\mathrm{i}v_f\frac{\partial}{\partial x}\right)G^{\mathrm{I,I}}_{\uparrow 1}(x,\tau;x',\tau')=\delta(\tau-\tau')\delta(x-x') - \lambda\delta(x)[G^{\mathrm{I,I}}_{\uparrow 1}(x,\tau;x',\tau')+\mathrm{i}G^{\mathrm{II,I}}_{\uparrow 1}(x,\tau;x',\tau')], \tag{28}$$

and

$$\left(\frac{\partial}{\partial\tau}+\mathrm{i}v_f\frac{\partial}{\partial x}\right)G^{\mathrm{II,I}}_{\uparrow 1}(x,\tau;x',\tau')=-\lambda\delta(x)[G^{\mathrm{II,I}}_{\uparrow 1}(x,\tau;x',\tau')-\mathrm{i}G^{\mathrm{I,I}}_{\uparrow 1}(x,\tau;x',\tau')]. \tag{29}$$

Equations (28), (29) have to be supplemented with the set of equations of motion for $G^{\mathrm{II,II}}_{\uparrow 1}$ and for $G^{\mathrm{I,II}}_{\uparrow 1}$, with the replacement $\mathrm{i}\to-\mathrm{i}$.

The detailed solution of equations (28), (29) is provided in appendix B. The S-matrix will come out to be diagonal with respect to any index but the representation index, according to the definition:

$$G^{a,b}_{\sigma\alpha}(\mathrm{i}\omega_{\mathrm{m}};x>0>x')=\sum_c S^{a,c}_{\sigma\alpha}(\mathrm{i}\omega_{\mathrm{m}})G^{c,b}_{\sigma\alpha}(\mathrm{i}\omega_{\mathrm{m}};0>x>x'), \tag{30}$$

where ω_{m} are the Matsubara frequencies.

From the results of appendix B, we find:

$$\begin{aligned} S^{\mathrm{I,I}}_{\uparrow 1}(\mathrm{i}\omega_{\mathrm{m}}) &= 1+2\pi\mathrm{i}\frac{\lambda}{1+2\lambda\mathcal{F}(\mathrm{i}\omega_{\mathrm{m}})} \\ S^{\mathrm{II,I}}_{\uparrow 1}(\mathrm{i}\omega_{\mathrm{m}}) &= 2\pi\frac{\lambda}{1+2\lambda\mathcal{F}(\mathrm{i}\omega_{\mathrm{m}})} \end{aligned} \tag{31}$$

$$S^{\mathrm{II,II}}_{\uparrow 1}(\mathrm{i}\omega_{\mathrm{m}})=S^{\mathrm{I,I}}_{\uparrow 1}(\mathrm{i}\omega_{\mathrm{m}}),\qquad S^{\mathrm{I,II}}_{\uparrow 1}(\mathrm{i}\omega_{\mathrm{m}})=-S^{\mathrm{II,I}}_{\uparrow 1}(\mathrm{i}\omega_{\mathrm{m}}). \tag{32}$$

Going back to real time, we get:

$$\mathcal{F}(\mathrm{i}\omega_{\mathrm{m}}\to\omega+\mathrm{i}\eta)=-\mathrm{i}\pi\left(1-\frac{\mathrm{i}}{\pi}\ln\left[\frac{D-\omega}{D+\omega}\right]\right),$$

where D is a band cutoff energy.

Finally

$$\begin{aligned} S^{\mathrm{I,I}}_{\uparrow 1}(\omega)=S^{\mathrm{II,II}}_{\uparrow 1}(\omega)&=\frac{1-2\lambda\ln\left[\frac{D-\omega}{D+\omega}\right]}{1-2\pi\mathrm{i}\lambda-2\lambda\ln\left[\frac{D-\omega}{D+\omega}\right]}, \\ S^{\mathrm{II,I}}_{\uparrow 1}(\omega)=-S^{\mathrm{I,II}}_{\uparrow 1}(\omega)&=\frac{2\pi\lambda}{1-2\pi\mathrm{i}\lambda-2\lambda\ln\left[\frac{D-\omega}{D+\omega}\right]}. \end{aligned} \tag{33}$$

This S-matrix is perfectly unitary in the representation space. The unitary limit is achieved with $\lambda\to\infty$. In this limit, the on-shell S matrix in the (I, II) space, $\mathbf{S}_{\sigma\alpha}(\omega=0)$, is given by:

$$\mathbf{S}_{\sigma\alpha}(\omega=0)=\begin{pmatrix}0 & -\mathrm{i}(\sigma\alpha)\\ \mathrm{i}(\sigma\alpha) & 0\end{pmatrix}. \tag{34}$$

According to the definition of phase shift δ for elastic scattering, $S=\mathrm{e}^{2\mathrm{i}\delta}$, we obtain the corresponding phase shift in the various channels, in the unitarity limit, given by $\delta^{\mathrm{I\,II}}_{\uparrow 1}(\omega=0)=-\frac{\pi}{4}$, $\delta^{\mathrm{II\,I}}_{\uparrow 1}(\omega=0)=\frac{\pi}{4}$. In the one channel spin-1/2 Kondo effect, the phase shift is $\delta_\sigma=\frac{\pi}{2}$.

The appearance of matrix elements that are off-diagonal in the representation index avoids the unitarity paradox, at the price of alleging scattering processes swapping the representation, corresponding to changing the spin-flavour quantum number by ± 2.

The derivation above also provides the boundary conditions for the bosonic fields Ψ_X ($X = \mathrm{ch}, \mathrm{sp}, \mathrm{fl}, \mathrm{sf}$) at the origin. As x crosses the location of the scattering centre ($x = 0$), none of the field changes, but Ψ_{sf}, according to:

$$\Psi_{\mathrm{sf}}(x) \to -\Psi_{\mathrm{sf}}(x) + \pi. \tag{35}$$

In the following sections, we abandon the I, II-representation, and define the physical conduction states in fermionic coordinates. To do so, we must derive the irrelevant operators providing the leading corrections to the $T = 0$ limit of the scattering dynamics.

5. The first irrelevant correction to the fixed-point Hamiltonian, physical states and the unitary limit of the conductance

In the previous sections, when bosonizing the fermionic fields, we stressed the representation redundancy associated with the spin-flavour quantum number. Such a redundancy does not affect the physical validity of the bosonization procedure, as both representations possess the same observable quantum numbers. However, it must be taken care of, somehow, when characterizing the fermionic Fock space for delocalized particles. To recognize what the physical fermionic conduction states are, we have to discuss the first irrelevant correction to the fixed point Hamiltonian $H_{\lambda}^{\mathrm{2CK}}$ in equation (26). In order to do so, we will first go back to bosonic coordinates, and then derive the first irrelevant correction to the bosonic fixed point Hamiltonian $H_{\mathrm{K}}^{\mathrm{2CK}}$ of equation (4), by building the perturbation theory about the fixed point, that is, by assuming the boundary conditions in equation (35), and by applying the Schrieffer–Wolff procedure to compute the various operators.

Irrelevant corrections arise when the kinetic energy term is added to $H_{\mathrm{K}}^{\mathrm{2CK}}$, and high energy states with a localized triplet at the impurity are alleged to take part in the scattering process as virtual states (each singlet state has an energy $E_{\mathrm{S}} = -9J/4$, and each triplet one has energy $E_{\mathrm{T}} = 7J/4$, see appendix C for details).

To start the derivation, let us notice that, as we show in equation (14), the Kondo interaction Hamiltonian only contains spin and spin-flavour bosonic fields. Therefore, we may factorize out both charge and flavour fields, and write the kinetic energy in the 'reduced' bosonized form:

$$H_{\mathrm{Red}} = \frac{v_f}{4\pi}\left[\int \mathrm{d}x \sum_{X=\mathrm{sp,sf}} \left(\frac{\mathrm{d}\Psi_X}{\mathrm{d}x}(x)\right)^2\right]. \tag{36}$$

This factorization might be thought of as an artifact of the long-wavelength expansion, and it may be possible that, during the renormalization procedure, some terms arise, coupling charge and flavour to the remaining degrees of freedom. However, we will assume that such terms are irrelevant anyway at low enough temperature.

Using the Schrieffer–Wolff procedure, we take as the lowest-energy subspace the one spanned by the singlets $|\mathrm{Sin}, A, \{\Xi\}\rangle$, $|\mathrm{Sin}, B, \{\Xi\}\rangle$, and we construct an effective Hamiltonian as a perturbative expansion in t^2/J. Defining the projector onto the lowest-energy subspace as:

$$\mathbf{P}_0 = \sum_{u=A,B} |\mathrm{Sin}, u, \{\Xi\}\rangle\langle \mathrm{Sin}, u, \{\Xi\}|, \tag{37}$$

the effective Hamiltonian, up to terms $\mathcal{O}(t^3/J^2)$, is:

$$H_{\mathrm{Eff}} \approx \mathbf{P}_0(H_{\mathrm{Red}} + H_{\mathrm{K}})\mathbf{P}_0 + \mathbf{P}_0\left\{\frac{1}{E_{\mathrm{S}} - E_{\mathrm{T}}}[H_{\mathrm{Red}}[\mathbf{1} - \mathbf{P}_0]H_{\mathrm{Red}}] + \left(\frac{1}{E_{\mathrm{S}} - E_{\mathrm{T}}}\right)^2 [H_{\mathrm{Red}}[\mathbf{1} - \mathbf{P}_0]H_{\mathrm{Red}}[\mathbf{1} - \mathbf{P}_0]H_{\mathrm{Red}}]\right\}\mathbf{P}_0. \tag{38}$$

In this section we focus on the first term on the rhs of equation (38), $\mathbf{P}_0(H_{\rm Red} + H_{\rm K})\mathbf{P}_0$. In appendix C, we derive the action of $H_{\rm Red}$ in the discrete lattice model, where $H_{\rm Red}$ is substituted by the corresponding lattice operator, $H_{\rm T,Red}$ (see appendix C for details). When computing matrix elements of $H_{\rm T,Red}$ between different impurity states, we include only the impurity neighbouring sites (which is equivalent in spirit to Wilson's NRG approach), and use the symbol $h_{\rm T}$ when referring to the corresponding operator. We show that, once projected on the space of the singlets, the corresponding hopping term takes the form:

$$\mathbf{P}_0 H_{\rm Red}\mathbf{P}_0 \to -\tfrac{1}{2}t\mathcal{Q}_0(\mathcal{Q}_a + \mathcal{Q}_{-a})\mathcal{Q}_0. \tag{39}$$

When written in terms of fermionic fields, the operator in equation (39) contains contributions that are off-diagonal in the I, II representation. However, in the continuum limit $a \to 0$, such terms just add up to the scattering potential in equation (26), so that they can be accounted for by substituting $\lambda \to \lambda - t$. This has no consequence on the developments of section 4, because $\lambda \to \infty$ at the end, but shows that states I and II have to be properly mixed by hopping at any distance from the impurity.

We recognize that the corresponding physical requirement is that $\mathcal{Q}_x$ commutes with the Hamiltonian not just at the origin, but at any point x. Hence, physical states can be constructed by using the projection operators given by:

$$\mathcal{P}_\pm = \frac{1}{\sqrt{2}}\prod_x(\mathbf{1}_x \pm \mathcal{Q}_x) \tag{40}$$

and by requiring that physical one-particle states are unaffected under, for instance, application of $\mathcal{P}_+$. These states are given by:

$$|\text{phys}+, \sigma\alpha\rangle_x = \frac{1}{\sqrt{2}}[c^{\dagger,\text{I}}_{\sigma\alpha}(x) - \text{i}(\sigma\alpha)c^{\dagger,\text{II}}_{\sigma\alpha}(x)]|0\rangle. \tag{41}$$

(The other set of one-particle physical states, $|\text{phys}-, \sigma\alpha\rangle_x$, is obtained by changing $\text{i} \to -\text{i}$.)

Therefore, the transformation matrix $\mathbf{U}$ that maps the I, II-representation onto the basis of the physical states, is:

$$\mathbf{U} = \begin{pmatrix} 1/\sqrt{2} & -\text{i}/\sqrt{2} \\ 1/\sqrt{2} & \text{i}/\sqrt{2} \end{pmatrix}.$$

$\mathbf{U}$ transforms the $\mathbf{S}$ matrix of equation (34) as follows:

$$\mathbf{U}^\dagger\mathbf{S}_{\sigma\alpha}\mathbf{U} = \begin{pmatrix} -1 & 0 \\ 0 & 0 \end{pmatrix}. \tag{42}$$

As we have projected onto just one of the two possible sets of physical even symmetry states, we find an $\mathbf{S}$ matrix for the even states which has just one non-vanishing element (that is -1, implying that also the even wavefunction has a node at the origin, as it must be in the unitary limit). The other possible physical states decouple from the scattering dynamics. Had we chosen the other set of states, the transformed matrix would have, instead, only the bottom diagonal element different from 0.

At this point we have to recall that this result refers to the even-parity wave. In fact, we get full transmission for both parities $l = \text{e}, \text{o}$, because the S-matrix is diagonal in the basis of physical states, and the matrix elements are given by $\mathbf{S}^{(+),l} = -\mathbf{1}$, for both parities $l = (\text{e}, \text{o})$. The transmission across the impurity is given by the trace [35]:

$$\mathbf{T} = \text{Tr}_{(+)}\left\{\left|\tfrac{1}{2}\sum_l S^{(+),l}\right|^2\right\} = \text{Tr}_{(+)}\{1\}. \tag{43}$$

Here $\mathrm{Tr}_{(+)}$ means tracing over all physical degrees of freedom σ, α. Although the system possesses four degrees of freedom, they are shared by the two physical $\pm$-ground states. In fact, there is a $\mathbf{Z}_2$ symmetry breaking in this system. Hence $\mathrm{Tr}_{(+)}\{1\} = 2$.

By applying Landauer formula to equation (43), we obtain the correct conductivity in the unitary limit:

$$\tilde{G} = \frac{e^2}{h}\frac{1}{2}\mathrm{Tr}_{(+)}\left\{\left|\frac{1}{2}\sum_l S^{(+),l}\right|^2\right\} = \frac{2e^2}{h}. \tag{44}$$

This corresponds to the halving of the zero-point entropy of the ground state, which turns to be $1/2\ln(2)$ for each ground state.

The fractionalization of the degrees of freedom can be understood also within the (I, II) representation for the S-matrix given in equation (34). One can think of closing the line onto itself in a symmetrical ring geometry, with two equal impurities at opposite sites. In this representation, in the upper branch we have propagation of type-I forward scattering into type II across one impurity, while in the lower branch the scattering is back, II $\to$ I, across the other impurity. Each process gives rise to a phase shift at $\omega = 0$, given by $\delta^e = \pm\pi/4$. The conductance across each impurity is $\tilde{G} = 2 \times 2 \times \frac{e^2}{h}\sin^2\delta^e = 2\frac{e^2}{h}$, where the first factor comes from the spin degrees of freedom, while the second one comes from the number of channels. Thus, the unitary limit is again obtained.

6. Leading finite-T corrections to the unitary conductance

In this section we will explicitly write down finite-T corrections to the fixed point conductance, coming from higher-order corrections to the fixed point Hamiltonian, (that is, from operators arising in the perturbative expansion of equation (38)). In appendix C we derive term by term the contributions to equation (38), up to third order. The matrix elements of the various operators in the basis of the singlets $|\mathrm{Sin}, u, \{\Xi\}\rangle$, $(u = A, B)$ form a 2×2 operator matrix, acting on the two low-energy singlets. Eventually, we will restrict them to the subset of physical states defined in the previous section.

In particular, in this section we will derive finite-frequency contributions to the fermionic S-matrix. These will come out to be $\propto\sqrt{\omega}$, which shows the NFL-nature of the corresponding ground state [11]. Vertex corrections provide higher-order contributions, which we will not consider here.

Following the derivation of appendix C, we see that, to $\mathcal{O}(t^2/J)$, we obtain the following matrix elements:

$$M^2_{AB} = M^2_{BA} = 0; \qquad M^2_{AA} = M^2_{BB} = \frac{2t^2}{E - \frac{7}{4}J} \approx -\frac{t^2}{2J}. \tag{45}$$

These terms provide just an over-all trivial shift of each energy eigenvalue by a constant amount $\mathcal{O}(t^2)$. Non-trivial effects, instead, arise from the third-order corrections.

From the calculations reported in appendix C, we see that:

$$M^3_{AA} = M^3_{BB} = 0; \qquad M^3_{AB} = \frac{t^3}{\pi J^2}\sin[\Psi_{\mathrm{sf}}(0)]\frac{\mathrm{d}\Psi_{\mathrm{sp}}(0)}{\mathrm{d}x} \tag{46}$$

plus terms $\mathcal{O}(t^2/J)$ (and higher) that renormalize the ones considered before.

The third-order correction in equation (46) is not affected by the physicality constraint because of the operational relation: $[\prod_x \mathcal{Q}_x, \sin[\Psi_{\mathrm{sf}}(x)]] = 0$. Since M^3 changes by ± 1 the spin-flavour, the corresponding diagonal (in I, II) contributions to the fixed-point Green

functions will be zero. Instead, it gives an $\mathcal{O}(t^3/J^2)$ off-diagonal correction to $G^{\mathrm{I,II}}_{\uparrow 1}$. In the interaction representation it reads:

$$\delta G^{\mathrm{I,II}}_{\sigma\alpha,\sigma'\alpha'}(x,\tau;x',\tau') = \int_0^\beta \mathrm{d}\tau_1 \mathrm{Tr}\{\mathrm{e}^{-\beta H_0} T_\tau [\phi^{\mathrm{I}}_{\sigma\alpha}(x,\tau) W_{\mathrm{Int}}(\tau_1) \phi^{\dagger,\mathrm{II}}_{\sigma\alpha}(x',\tau')]\} \delta_{\sigma\sigma'}\delta_{\alpha\alpha'}. \tag{47}$$

Computing the trace of equation (47) requires using the bosonic representation for the operators $\phi^{\mathrm{I,II}}$ provided in equation (22). In bosonic coordinates, $W_{\mathrm{Int}}(\tau_1)$ is defined as:

$$W_{\mathrm{Int}}(\tau_1) = \frac{t^3}{\pi J^2} \mathrm{e}^{\tau_1 H_{\mathrm{fp}}} \left\{ :\sin[\Psi_{\mathrm{sf}}(0)]: \frac{\mathrm{d}\Psi_{\mathrm{sp}}}{\mathrm{d}x}(0) \right\} \mathrm{e}^{-\tau_1 H_{\mathrm{fp}}}. \tag{48}$$

Two independent periods appear in the Green functions: the length L and the inverse temperature β. A rigorous calculation of the correlators in equation (47) would require the introduction of Jacobi's elliptic θ-functions. However, here we will attempt to compute just the finite-frequency corrections at $T = 0$. Therefore, we shall approximate equation (47) as:

$$\begin{aligned}\delta G^{\mathrm{I,II}}_{\sigma\alpha}(x,\tau;x',\tau') = \frac{t^3}{\pi J^2} \int_0^\infty \mathrm{d}\tau_1 \langle :\mathrm{e}^{-\frac{\mathrm{i}}{2}\Psi_{\mathrm{ch}}(x,\tau)}: :\mathrm{e}^{\frac{\mathrm{i}}{2}\Psi_{\mathrm{ch}}(x',\tau')}:\rangle \langle :\mathrm{e}^{-\alpha\frac{\mathrm{i}}{2}\Psi_{\mathrm{fl}}(x,\tau)}: :\mathrm{e}^{\alpha\frac{\mathrm{i}}{2}\Psi_{\mathrm{fl}}(x',\tau')}:\rangle \\ \times \left\langle :\mathrm{e}^{-\sigma\frac{\mathrm{i}}{2}\Psi_{\mathrm{sp}}(x,\tau)} \frac{\partial\Psi_{\mathrm{sp}}}{\partial x}(0,\tau_1) \mathrm{e}^{\sigma\frac{\mathrm{i}}{2}\Psi_{\mathrm{sp}}(x',\tau')}: \right\rangle \\ \times \langle :\mathrm{e}^{+\sigma\alpha\frac{\mathrm{i}}{2}\Psi_{\mathrm{sf}}(x,\tau)}: :\sin[\Psi_{\mathrm{sf}}(0,\tau_1)]: :\mathrm{e}^{-\sigma\alpha\frac{\mathrm{i}}{2}\Psi_{\mathrm{sf}}(x',\tau')}\rangle,\end{aligned} \tag{49}$$

where $\langle\cdots\rangle$ denotes ground state average. As shown in appendix D, for the case $\{\sigma\alpha\} = \{\uparrow 1\}$ and in the limit of $T = 0$ and large L, equation (49) provides the result:

$$\delta G^{\mathrm{I,II}}_{\uparrow 1}(\mathrm{i}\omega_{\mathrm{m}};x,x') = -\frac{t^3}{J^2 v_f^{\frac{3}{2}}} \sqrt{\frac{\omega}{\pi v_f}} \mathrm{e}^{\mathrm{i}\frac{\omega}{v_f}(x-x')} \tag{50}$$

with $x - x' > 0$. In equation (50), we have performed the analytic continuation to real frequencies for the retarded Green function: $\omega_{\mathrm{m}} \to -\mathrm{i}\omega$.

Introducing in equation (50) the Kondo temperature as the relevant physical energy scale according to the substitution: $\frac{t^3}{2\pi^{3/2} v_f J^2} \to \frac{1}{\sqrt{T_{\mathrm{K}}}}$, we obtain a leading finite-frequency correction that goes as $\omega^{\frac{1}{2}}$, in agreement with the results obtained in [11]. In particular, we have found a finite-ω correction to the S matrix given by:

$$\delta \mathbf{S}_{\sigma\alpha}(\omega) = \begin{bmatrix} 0 & \mathrm{i}(\sigma\alpha)\sqrt{\frac{|\omega|}{T_{\mathrm{K}}}} \\ -\mathrm{i}(\sigma\alpha)\sqrt{\frac{|\omega|}{T_{\mathrm{K}}}} & 0 \end{bmatrix}. \tag{51}$$

By projecting the result of equation (51) on the basis of physical states, we get:

$$\mathbf{U}^\dagger [\mathbf{S}_{\sigma\alpha} + \delta\mathbf{S}_{\sigma\alpha}]\mathbf{U} = \begin{bmatrix} -1 + \sqrt{\frac{|\omega|}{T_{\mathrm{K}}}} & 0 \\ 0 & 0 \end{bmatrix}. \tag{52}$$

As a side remark, let us consider the case of a QD hybridized to metal contacts by a tunnelling potential V. If we use the relations found within the Anderson model [37], we find the width of the Kondo resonance to be given by: $\Gamma = \frac{4k_{\mathrm{B}}T_{\mathrm{K}}}{\pi} = \pi\nu(0)|V|^2$, where V is the tunnelling strength and $\nu(0) = 2\pi/v_f$ is the density of states at the Fermi level. This implies, in our case, that $|V| = \frac{J^2}{t^3}\sqrt{2\pi v_f^3}$.

By using the result in equation (52), we compute the finite-energy transmission:

$$\mathbf{T}(\omega, T=0) = \mathrm{Tr}_{(+)}\left\{ \left| \frac{1}{2} \sum_l [S^{(+),l} + \delta S^{(+),l}] \right|^2 \right\} = 2\left(1 - \frac{1}{2}\left|\frac{\omega}{T_{\mathrm{K}}}\right|^{\frac{1}{2}}\right). \tag{53}$$

Finally, in order to obtain from equation (53) finite-temperature dependence of the conductance, we have to recall that, at finite temperatures, there are two contributions to the conductance: one arising from the smearing of the Fermi surface, the other from the inelastic processes. In fact, for the large U Anderson model, the explicit dependence of the transport time on temperature at the Fermi energy has to be taken into account separately [37]. This gives:

$$\tilde{G}(T) = \frac{e^2}{h}\int \mathrm{d}\omega\left(-\frac{\partial f(\omega)}{\partial\omega}\right)\mathbf{T}(\omega,T) = \frac{2e^2}{h}\beta\int_{-\mu}^{\infty}\mathrm{d}\omega\,\frac{\mathrm{e}^{\beta\omega}}{(1+\mathrm{e}^{\beta\omega})^2}\left[1-\frac{1}{2}\left|\frac{\omega}{T_{\mathrm{K}}}\right|^{\frac{1}{2}}\right]+\boldsymbol{\Delta}(\mu,T)$$
$$\approx \frac{2e^2}{h}\left[1-\sqrt{\frac{3\pi}{8}}\sqrt{\frac{T}{T_{\mathrm{K}}}}\right] \tag{54}$$

where $f(\omega)$ is the Fermi distribution, and $\boldsymbol{\Delta}$ is the total contribution coming from inelastic processes, which we neglect here, as it is assumed to provide corrections that are higher order than $\sqrt{T}$. Equation (54) contains the ultimate result of our derivation: the calculation of the fixed-point contribution to the conductance, together with the leading finite-T correction, and the elucidation of the connection between this correction and the various scattering processes that take place at the fixed point. As we have already mentioned, our formalism allows also for calculating the inelastic term arising from vertex corrections, but we will not consider them here.

7. Conclusions

In this paper, we use the Landauer formula to derive the conductance at the two channel spin $1/2$ overscreened Kondo fixed point, together with leading finite-temperature corrections. We perform our calculations within the framework of our simple Hamiltonian theory, in which we derive a suitable fermionic representation of the S-matrix, by using bosonization as an intermediate step. In order for us to achieve such apparently simple results, we had to go through various mathematical approaches, which are used in the literature to analyse different aspects of the overscreened Kondo problem [11, 27, 34]. For instance, we had to complement the regularization scheme introduced in [27] with the bosononization technique widely used in [11], and with the careful discussion about the role of the spin-flavour quantum number in [34].

Our research is motivated by the renewed interest in the Kondo model, which has recently arisen in connection with conductance experiments across QDs. In general, using simple models for correlated electrons, like the Anderson model, allows for grasping the physics involved in tunnelling experiments across confined areas between two contacts, as well as across Coulomb blockaded systems (like the QD device we have in mind). Recently, efforts have been made to achieve an exact description of transport also in the non-equilibrium case, starting from the integrability of the two-lead Anderson model [36], which confirms previous numerical RG results [23]. Despite the exactness of these results, they are unsuitable for our case, as they refer to the Fermi liquid 1CK fixed point.

Recently, various groups have been predicting that 2CK could be realized in QD systems. In particular, we have proposed that the orbital 2CK effect may arise in a vertical structure with cylindrical symmetry around an applied magnetic field [16].

In our proposal, the dynamical degrees of freedom involved in the scattering across the interacting dot are provided by an appropriate combination of the transverse angular momentum of lead electrons, m, and of their spin, σ. The single particle wavefunction of the delocalized electrons travelling along the z direction has an orbital part factorized in the cross-sectional

plane. In a linearized band picture and close to the Fermi energy ϵ_F, their wavefunction of energy ϵ and parity l w.r.t. $z = 0$ is:

$$\psi^l_{\epsilon\sim\epsilon_F,q,m,\sigma}(\rho,\theta;z) = (\operatorname{sgn} z)^l e^{i(k_F+q)|z|}\varphi_{\delta\approx 0,m}(\rho)e^{im\theta}\chi_\sigma, \tag{55}$$

where $\delta = \epsilon - \hbar v_F|q|$, and χ_σ is the spin wavefunction.

Another proposal is based on the use of an additional lateral QD to tune the exchange coupling to the channels to the isotropic point [17]. In such a geometry, however, even a small anisotropy in the coupling to the channels is enough to drive, at low enough T, the system from the 2CK fixed point to a 1CK channel fixed point, with strong coupling only in the dominant channel [38]. This problem does not arise in [16], because of the assumed cylindrical symmetry. This symmetry does not allow for any off-diagonal coupling mixing the two channels, because it enforces the angular momentum selection rule in the cross plane. Of course it is very demanding to produce such a strictly cylindrical system experimentally.

These proposals have triggered a renewed interest in 2CK transport. On the theoretical side, reconsideration of the matter is relevant in view of the particular kind of devices involved in the proposed experiments. Indeed, the scattering approach used in [11], in conjunction with CFT techniques, is better suited for the single impurity s-wave scattering in a three-dimensional medium than for a two-lead device. In [18], the authors identify the two-channel Kondo fixed point as a quantum critical point between two Fermi liquid phases, and derive its dependance on external parameters such as temperature, magnetic field and voltage bias accordingly.

For the purpose of understanding the physics of the transport across mesoscopic devices, we believe our approach to be a straight connection between the physics of the overscreened Kondo problem at the fixed point and its physical consequences. In a clear and easy-to-follow framework that extends Nozières' hypothesis, it sheds light on the physical processes that happen at the impurity as $T \to 0$, and relates them to the macroscopically detectable non-Fermi liquid behaviour in the T-dependence of the conductance. The GS at the NFL fixed point is found to be degenerate. Because the physical system only involves one of these GSs and its corresponding excitations, the contribution of each degree of freedom to the conductance is halved. As discussed in section 4, this leads to the same unitary limit of the conductance as in the one channel case. Finally, our approach might also provide an alternative route to investigate the effect of anisotropy on the conductance.

Acknowledgments

We acknowledge fruitful discussions with M Fabrizio, P Wiegmann and I Aleiner. This work was partially supported by the TMR Project, contract FMRX-CT98-0180.

Appendix A. Basic bosonization steps

In this appendix we will review some basic bosonization steps, which will allow us to write down fermionic fields in terms of bosonic operators.

In order to write fermionic fields in bosonic coordinates, let us introduce a massless scalar bosonic field $\Psi(x)$, given by:

$$\Psi(x) = q + \frac{2\pi}{L}px + i\sum_{n\neq 0}\frac{\alpha_n}{n}e^{-\frac{2\pi i}{L}(nx - i|n|\frac{\eta}{2})} \tag{A.1}$$

where $\eta \equiv 0^+$ is a regularizer.

The algebra of the bosonic modes is:

$$[q, p] = i; \qquad [\alpha_n, \alpha_m] = n\delta_{n+m,0}. \tag{A.2}$$

Therefore, we may split $\Psi(x)$ into a creation and an annihilation part, $\Psi(x) = \Psi_+(x) + \Psi_-(x)$, with

$$\Psi_+(x) = q - \mathrm{i}\sum_{n=1}^{\infty}\frac{\alpha_{-n}}{n}\mathrm{e}^{\frac{2\pi \mathrm{i}n}{L}x - \frac{\pi n}{L}\eta}; \qquad \Psi_-(x) = \frac{2\pi x}{L}p + \mathrm{i}\sum_{n=1}^{\infty}\frac{\alpha_n}{n}\mathrm{e}^{\frac{-2\pi \mathrm{i}n}{L}x - \frac{\pi n}{L}\eta} \tag{A.3}$$

and

$$[\Psi_-(y), \Psi_+(x)] = -\ln(\mathrm{e}^{\frac{2\pi \mathrm{i}n}{L}y} - \mathrm{e}^{\frac{2\pi \mathrm{i}n}{L}(x+\mathrm{i}\eta)}). \tag{A.4}$$

The ground state of the Fock space spanned by the bosonic modes, $|\mathrm{bvac}\rangle$, is defined by:

$$p|\mathrm{bvac}\rangle = \alpha_n|\mathrm{bvac}\rangle = 0 \qquad (n > 0). \tag{A.5}$$

A fermionic field may be defined as

$$c^{\dagger}(x) = :\mathrm{e}^{\mathrm{i}\Psi(x)}: \tag{A.6}$$

where the columns : : denote normal ordering with respect to $|\mathrm{bvac}\rangle$.

Indeed, by using the general identity

$$\mathrm{e}^{A}\mathrm{e}^{B} = \mathrm{e}^{B}\mathrm{e}^{A}\mathrm{e}^{[A,B]},$$

which holds if $[A, B]$ is a number, one gets:

$$:\mathrm{e}^{\mathrm{i}\alpha\Psi(x)}::\mathrm{e}^{-\mathrm{i}\beta\Psi(y)}: = \mathrm{e}^{\mathrm{i}[\alpha\Psi_+(x)-\beta\Psi_+(y)]}\mathrm{e}^{\mathrm{i}[\alpha\Psi_-(x)-\beta\Psi_-(y)]}\left[\frac{1}{(\mathrm{e}^{\frac{2\pi \mathrm{i}}{L}x} - \mathrm{e}^{\frac{2\pi \mathrm{i}}{L}(y+\mathrm{i}\eta)})^{\alpha\beta}}\right]. \tag{A.7}$$

As $\alpha, \beta = \pm 1$ and $x \neq y$, we get:

$$c(x)c(y) + c(y)c(x) = c(x)c^{\dagger}(y) + c^{\dagger}(y)c(x) = 0. \tag{A.8}$$

On the other hand, by properly regularizing the anticommutator, while as $x \to y$ the anticommutator between $c(x)$ and $c(y)$ remains equal to 0 (as well as the anticommutator between $c^{\dagger}(x)$ and $c^{\dagger}(y)$), one gets:

$$c(x)c^{\dagger}(y) + c^{\dagger}(y)c(x) = \delta\left[\frac{x-y}{L}\right]. \tag{A.9}$$

The density operator at a point x may be expressed in bosonic coordinates by means of the 'point-splitting regularization' as follows:

$$\rho(x) = \lim_{y\to x}:\{:\mathrm{e}^{\mathrm{i}\Psi(y)}::\mathrm{e}^{-\mathrm{i}\Psi(x)}:\}: = \frac{1}{2\pi}\frac{\mathrm{d}\Psi(x)}{\mathrm{d}x}. \tag{A.10}$$

The free kinetic Hamiltonian may also be written in a bosonized form as follows:

$$H_{\mathrm{T}} = -\mathrm{i}v_f\int \mathrm{d}x:\mathrm{e}^{\mathrm{i}\Psi_+(x)}\mathrm{e}^{\mathrm{i}\Psi_-(x)}\frac{\mathrm{d}}{\mathrm{d}x}[\mathrm{e}^{-\mathrm{i}\Psi_+(x)}\mathrm{e}^{-\mathrm{i}\Psi_-(x)}]: = \frac{v_f}{4\pi}\int \mathrm{d}x\left[\frac{\mathrm{d}\Psi(x)}{\mathrm{d}x}\right]^2. \tag{A.11}$$

When fermions carry several quantum numbers (spin, flavour), bosonizing requires first of all introducing many bosonic fields Ψ_X. Also, in order to make fermions with different quantum numbers anticommute, one has to introduce a 'Klein factor' $\eta_{\sigma\alpha}$ in front of each bosonized field. In general, one chooses $\eta_{\sigma\alpha}$ to be a real Majorana fermion, that is, $(\eta_{\sigma,\alpha})^2 = 1$ [19]. As a consequence, fermionic operators defined as

$$\begin{aligned} c_{\sigma\alpha}(x) &= \eta_{\sigma\alpha}:\mathrm{e}^{-\frac{\mathrm{i}}{2}[\Psi_{\mathrm{ch}}(x)+\sigma\Psi_{\mathrm{sp}}(x)+\alpha\Psi_{\mathrm{fl}}(x)+\alpha\sigma\Psi_{\mathrm{sf}}(x)]}:; \\ c^{\dagger}_{\sigma\alpha}(x) &= \eta_{\sigma\alpha}:\mathrm{e}^{\frac{\mathrm{i}}{2}[\Psi_{\mathrm{ch}}(x)+\sigma\Psi_{\mathrm{sp}}(x)+\alpha\Psi_{\mathrm{fl}}(x)+\alpha\sigma\Psi_{\mathrm{sf}}(x)]}: \end{aligned} \tag{A.12}$$

anticommute with each other for different quantum numbers, as they must do.

The following commutation relation holds:

$$\left[\frac{1}{2\pi}\frac{\mathrm{d}\Psi(x)}{\mathrm{d}x}, :\mathrm{e}^{\mathrm{i}\alpha\Psi(y)}:\right] = \alpha\delta(x-y):\mathrm{e}^{\mathrm{i}\alpha\Psi(y)}:. \tag{A.13}$$

By using only one bosonic field $\Psi(x)$ it is possible to build an $SU(2)$ spin-current $\vec{j}(x)$. The components of the vector current density are given by:

$$j_{\pm}(x) = \frac{1}{\sqrt{2}}:\mathrm{e}^{\pm\mathrm{i}\sqrt{2}\Psi(x)}:; \qquad j_z(x) = \frac{1}{2\pi}\frac{\mathrm{d}\Psi}{\mathrm{d}x}(x). \tag{A.14}$$

Indeed, according to equation (A.7), in the case $\alpha = \beta = \sqrt{2}$, and to equation (A.13), we obtain:

$$[j_+(x), j_-(y)] = \mathrm{i}\frac{L}{2\pi}\delta'(x-y) + \delta(x-y)j^z(y) \tag{A.15}$$

and

$$[j^z(x), j^{\pm}(y)] = \pm\delta(x-y)j^{\pm}(y). \tag{A.16}$$

Equations (A.15), (A.16) provide us with the usual $SU(2)$ affine algebra obeyed by the spin-density operator.

This, in particular, proves that the operators $\vec{\Sigma}_A(x)$ and $\vec{\Sigma}_B(x)$ we defined in section 3 are $SU(2)$ spin current operators.

The corresponding spinors at a point x may be created by acting $|\mathrm{bvac}\rangle$ with $:\mathrm{e}^{\pm\frac{\mathrm{i}}{2}[\Psi_{\mathrm{sp}}+\Psi_{\mathrm{sf}}](x)}:$ and $:\mathrm{e}^{\pm\frac{\mathrm{i}}{2}[\Psi_{\mathrm{sp}}-\Psi_{\mathrm{sf}}](x)}:$, respectively. Let us define:

$$|\sigma;A\rangle_x \equiv [:\mathrm{e}^{\sigma\frac{\mathrm{i}}{2}[\Psi_{\mathrm{sp}}+\Psi_{\mathrm{sf}}](x)}:]|\mathrm{bvac}\rangle; \qquad |\sigma;B\rangle_x \equiv [:\mathrm{e}^{\sigma\frac{\mathrm{i}}{2}[\Psi_{\mathrm{sp}}-\Psi_{\mathrm{sf}}](x)}:]|\mathrm{bvac}\rangle. \tag{A.17}$$

The following commutation relations hold (either the upper or the lower signs hold):

$$[\Sigma_A^{\pm}(x), :\mathrm{e}^{\pm\frac{\mathrm{i}}{2}[\Psi_{\mathrm{sp}}+\Psi_{\mathrm{sf}}](y)}:] = [\Sigma_B^{\pm}(x), :\mathrm{e}^{\pm\frac{\mathrm{i}}{2}[\Psi_{\mathrm{sp}}-\Psi_{\mathrm{sf}}](y)}:] = 0 \tag{A.18}$$

and

$$\begin{aligned}[\Sigma_A^{\pm}(x), :\mathrm{e}^{\mp\frac{\mathrm{i}}{2}[\Psi_{\mathrm{sp}}+\Psi_{\mathrm{sf}}](y)}:] &= \delta(x-y):\mathrm{e}^{\pm\frac{\mathrm{i}}{2}[\Psi_{\mathrm{sp}}+\Psi_{\mathrm{sf}}](y)}:;\\ [\Sigma_B^{\pm}(x), :\mathrm{e}^{\mp\frac{\mathrm{i}}{2}[\Psi_{\mathrm{sp}}-\Psi_{\mathrm{sf}}](y)}:] &= \delta(x-y):\mathrm{e}^{\pm\frac{\mathrm{i}}{2}[\Psi_{\mathrm{sp}}-\Psi_{\mathrm{sf}}](y)}:.\end{aligned} \tag{A.19}$$

Finally

$$\begin{aligned}[\Sigma_A^{z}(x), :\mathrm{e}^{\pm\frac{\mathrm{i}}{2}[\Psi_{\mathrm{sp}}+\Psi_{\mathrm{sf}}](y)}:] &= \pm\tfrac{1}{2}\delta(x-y):\mathrm{e}^{\pm\frac{\mathrm{i}}{2}[\Psi_{\mathrm{sp}}+\Psi_{\mathrm{sf}}](y)}:;\\ [\Sigma_B^{z}(x), :\mathrm{e}^{\pm\frac{\mathrm{i}}{2}[\Psi_{\mathrm{sp}}-\Psi_{\mathrm{sf}}](y)}:] &= \pm\tfrac{1}{2}\delta(x-y):\mathrm{e}^{\pm\frac{\mathrm{i}}{2}[\Psi_{\mathrm{sp}}-\Psi_{\mathrm{sf}}](y)}:.\end{aligned} \tag{A.20}$$

The set of equations listed above shows that the doublet $|\sigma, A\rangle$ provides a spinor representation of the $SU(2)$ group generated by $\vec{\Sigma}_A$, and that the doublet $|\sigma, B\rangle$ provides a spinor representation of the $SU(2)$ group generated by $\vec{\Sigma}_B$.

To conclude this appendix, let us now prove that fermionic fields belonging to two different representations anticommuting with each other.

Let us start from the fields in the two representations expressed in bosonic coordinates:

$$\phi^{\mathrm{I}}_{\sigma\alpha}(x) = \eta_{\sigma\alpha}:\mathrm{e}^{-\frac{\mathrm{i}}{2}[\Psi_{\mathrm{ch}}(x)+\sigma\Psi_{\mathrm{sp}}(x)+\alpha\Psi_{\mathrm{fl}}(x)+\alpha\sigma\Psi_{\mathrm{sf}}(x)]}: \tag{A.21}$$

and

$$\phi^{\mathrm{II}}_{\sigma\alpha}(x) = \eta_{\sigma\alpha}:\mathrm{e}^{-\frac{\pi\mathrm{i}}{2}\tilde{N}_{\sigma\alpha}}\mathrm{e}^{-\frac{\mathrm{i}}{2}[\Psi_{\mathrm{ch}}(x)+\sigma\Psi_{\mathrm{sp}}(x)+\alpha\Psi_{\mathrm{fl}}(x)-\alpha\sigma\Psi_{\mathrm{sf}}(x)]}:, \tag{A.22}$$

where the Klein factors $\eta_{\sigma\alpha}$ are given by real Majorana variables.

Clearly, fields within the same representation anticommute:

$$\{\phi^{A}_{\sigma\alpha}(x), \phi^{A\dagger}_{\sigma',\alpha'}(y)\} = \delta_{\sigma\sigma'}\delta_{\alpha\alpha'}\delta(x-y). \tag{A.23}$$

Let us, now, consider fields from the two different representations. Let us start with two annihilation field operators (in the case $\{\sigma\alpha\} \neq \{\sigma'\alpha'\}$):

$$\{\phi^{\mathrm{I}}_{\sigma\alpha}(x), \phi^{\mathrm{II}}_{\sigma'\alpha'}(y)\} = \eta_{\sigma\alpha}\eta_{\sigma'\alpha'}\{\mathrm{e}^{-\frac{\mathrm{i}\pi}{4}[1+\sigma\sigma'+\alpha\alpha'-\sigma\sigma'\alpha\alpha']}[\mathrm{e}^{\frac{2\pi\mathrm{i}x}{L}} - \mathrm{e}^{\frac{2\pi\mathrm{i}y}{L}}]^{\frac{1}{4}[1+\sigma\sigma'+\alpha\alpha'-\sigma\sigma'\alpha\alpha']}$$
$$- [\mathrm{e}^{\frac{2\pi\mathrm{i}y}{L}} - \mathrm{e}^{\frac{2\pi\mathrm{i}x}{L}}]^{\frac{1}{4}[1+\sigma\sigma'+\alpha\alpha'-\sigma\sigma'\alpha\alpha']}\}$$
$$\times :\exp\Bigg[-\frac{\mathrm{i}}{2}[\Psi_{\mathrm{ch}}(x) + \Psi_{\mathrm{ch}}(y) + \sigma\Psi_{\mathrm{sp}}(x) + \sigma'\Psi_{\mathrm{sp}}(y)$$
$$+ \alpha\Psi_{\mathrm{fl}}(x) + \alpha'\Psi_{\mathrm{fl}}(y) - \alpha\sigma\Psi_{\mathrm{sf}}(x) - \alpha'\sigma'\Psi_{\mathrm{sf}}(y)]\Bigg]: = 0. \tag{A.24}$$

By following the same procedure, we obtain the result:

$$\{\phi^{\mathrm{I}\dagger}_{\sigma\alpha}(x), \phi^{\mathrm{II}\dagger}_{\sigma'\alpha'}(y)\} = 0 \tag{A.25}$$

and the anticommutation relations:

$$\{\phi^{\mathrm{I}}_{\sigma\alpha}(x), \phi^{\mathrm{II}\dagger}_{\sigma'\alpha'}(y)\} = \eta_{\sigma\alpha}\eta_{\sigma'\alpha'}\{\mathrm{e}^{\frac{\mathrm{i}\pi}{4}[1+\sigma\sigma'+\alpha\alpha'-\sigma\sigma'\alpha\alpha']}[\mathrm{e}^{\frac{2\pi\mathrm{i}x}{L}} - \mathrm{e}^{\frac{2\pi\mathrm{i}y}{L}}]^{-\frac{1}{4}[1+\sigma\sigma'+\alpha\alpha'-\sigma\sigma'\alpha\alpha']}]$$
$$- [\mathrm{e}^{\frac{2\pi\mathrm{i}y}{L}} - \mathrm{e}^{\frac{2\pi\mathrm{i}x}{L}}]^{-\frac{1}{4}[1+\sigma\sigma'+\alpha\alpha'-\sigma\sigma'\alpha\alpha']}]\}$$
$$\times :\exp\Bigg[-\frac{\mathrm{i}}{2}[\Psi_{\mathrm{ch}}(x) - \Psi_{\mathrm{ch}}(y) + \sigma\Psi_{\mathrm{sp}}(x) - \sigma'\Psi_{\mathrm{sp}}(y)$$
$$+ \alpha\Psi_{\mathrm{fl}}(x) - \alpha'\Psi_{\mathrm{fl}}(y) - \alpha\sigma\Psi_{\mathrm{sf}}(x) + \alpha'\sigma'\Psi_{\mathrm{sf}}(y)]\Bigg]: = 0 \tag{A.26}$$

and

$$\{\phi^{\mathrm{I}\dagger}_{\sigma\alpha}(x), \phi^{\mathrm{II}}_{\sigma'\alpha'}(y)\} = 0, \tag{A.27}$$

that complete the proof of the identities used throughout the paper.

Appendix B. Calculation of the fixed point Green functions

In this appendix we will show in detail how to calculate the fixed point Green functions with the method of the equations of motion. Within our framework, this will come out to be a straightforward application of one-dimensional scattering theory.

The equations of motion for $G^{\mathrm{I,I}}_{\uparrow 1}$ and $G^{\mathrm{II,I}}_{\uparrow 1}$ are reported in section 4 and are given by:

$$\left(\frac{\partial}{\partial\tau} - \mathrm{i}v_f\frac{\partial}{\partial x}\right)G^{\mathrm{I,I}}_{\uparrow 1}(x,\tau;x',\tau') = \delta(\tau-\tau')\delta(x-x')$$
$$- \lambda\delta(x)[G^{\mathrm{I,I}}_{\uparrow 1}(x,\tau;x',\tau') + \mathrm{i}G^{\mathrm{II,I}}_{\uparrow 1}(x,\tau;x',\tau')] \tag{B.1}$$

and

$$\left(\frac{\partial}{\partial\tau} - \mathrm{i}v_f\frac{\partial}{\partial x}\right)G^{\mathrm{II,I}}_{\uparrow 1}(x,\tau;x',\tau') = -\lambda\delta(x)[G^{\mathrm{II,I}}_{\uparrow 1}(x,\tau;x',\tau') - \mathrm{i}G^{\mathrm{I,I}}_{\uparrow 1}(x,\tau;x',\tau')]. \tag{B.2}$$

To solve the set of equations (B.1), (B.2), let us introduce the Green functions in the mixed representation:

$$G^{AB}_{\uparrow 1}(x,\tau;x',\tau') = \frac{1}{\beta}\sum_{\mathrm{i}\omega_{\mathrm{m}}}\int \mathrm{d}p\,\mathrm{e}^{-\mathrm{i}\omega_{\mathrm{m}}\tau}\mathrm{e}^{\mathrm{i}px}G^{AB}_{\uparrow 1}(\mathrm{i}\omega_{\mathrm{m}},p;x'). \tag{B.3}$$

In the mixed representation, the equations of motion become:

$$(-\mathrm{i}\omega_{\mathrm{m}} + v_f p)G^{\mathrm{I,I}}_{\uparrow 1}(\mathrm{i}\omega_{\mathrm{m}},p;x') = \mathrm{e}^{-\mathrm{i}px'} - \lambda\int \mathrm{d}q\,[G^{\mathrm{I,I}}_{\uparrow 1}(\mathrm{i}\omega_{\mathrm{m}},q;x') + \mathrm{i}G^{\mathrm{II,I}}_{\uparrow 1}(\mathrm{i}\omega_{\mathrm{m}},q;x')] \tag{B.4}$$

and

$$(-\mathrm{i}\omega_{\mathrm{m}} + v_f p)G^{\mathrm{II,I}}_{\uparrow 1}(\mathrm{i}\omega_{\mathrm{m}}, p; x') = -\lambda \int \mathrm{d}q\, [G^{\mathrm{II,I}}_{\uparrow 1}(\mathrm{i}\omega_{\mathrm{m}}, q; x') - \mathrm{i}G^{\mathrm{I,I}}_{\uparrow 1}(\mathrm{i}\omega_{\mathrm{m}}, q; x')]. \tag{B.5}$$

The solution to the set of equations (B.4), (B.5) is given by:

$$G^{\mathrm{I,I}}_{\uparrow 1}(\mathrm{i}\omega_{\mathrm{m}}, p; x') = \frac{\mathrm{e}^{-\mathrm{i}px'}}{-\mathrm{i}\omega_{\mathrm{m}} + v_f p} - \frac{1}{-\mathrm{i}\omega_{\mathrm{m}} + v_f p}\left[\frac{\lambda'}{1 + 2\lambda'\mathcal{F}(\mathrm{i}\omega_{\mathrm{m}})}\right] v_f \int \mathrm{d}q \left(\frac{\mathrm{e}^{-\mathrm{i}qx'}}{-\mathrm{i}\omega_{\mathrm{m}} + v_f q}\right) \tag{B.6}$$

and by

$$G^{\mathrm{II,I}}_{\uparrow 1}(\mathrm{i}\omega_{\mathrm{m}}, p; x') = \frac{1}{-\mathrm{i}\omega_{\mathrm{m}} + v_f p}\left[\frac{\mathrm{i}\lambda'}{1 + 2\lambda'\mathcal{F}(\mathrm{i}\omega_{\mathrm{m}})}\right] \int \mathrm{d}q\, v_f \left(\frac{\mathrm{e}^{\mathrm{i}qx'}}{-\mathrm{i}\omega_{\mathrm{m}} + v_f q}\right) \tag{B.7}$$

where $\lambda' = \lambda/v_f$ and $\mathcal{F}(\mathrm{i}\omega_{\mathrm{m}})$ is defined as:

$$\mathcal{F}(\mathrm{i}\omega_{\mathrm{m}}) = v_f \int \mathrm{d}p\, \frac{1}{-\mathrm{i}\omega_{\mathrm{m}} + v_f p} = \ln\left[\frac{D + \mathrm{i}\omega_{\mathrm{m}}}{-D + \mathrm{i}\omega_{\mathrm{m}}}\right]. \tag{B.8}$$

In equation (B.8), D is a high-energy band cutoff.

In order to derive the S-matrix elements, in section 4 we use the real space Green functions for $x > 0$ and $x' < 0$ in the limit $\lambda' \to \infty$. In the case $\omega_{\mathrm{m}} > 0$ they are

$$G^{\mathrm{I,I}}_{\uparrow 1}(\mathrm{i}\omega_{\mathrm{m}}; x, x') = \int \mathrm{d}p\, \mathrm{e}^{\mathrm{i}px} G^{\mathrm{I,I}}_{\uparrow 1}(\mathrm{i}\omega_{\mathrm{m}}, p; x') = \frac{2\pi\mathrm{i}}{v_f}\theta(\omega_{\mathrm{m}})\left[1 - 2\pi\mathrm{i}\frac{1}{2\mathcal{F}(\mathrm{i}\omega_{\mathrm{m}})}\right]\mathrm{e}^{-\frac{\omega_{\mathrm{m}}}{v_f}(x-x')} \tag{B.9}$$

and

$$G^{\mathrm{II,I}}_{\uparrow 1}(\mathrm{i}\omega_{\mathrm{m}}; x, x') = \int \mathrm{d}p\, \mathrm{e}^{\mathrm{i}px} G^{\mathrm{II,I}}_{\uparrow 1}(\mathrm{i}\omega_{\mathrm{m}}, p; x') = \frac{2\pi\mathrm{i}}{v_f}\theta(\omega_{\mathrm{m}})\left[2\pi\mathrm{i}\frac{\mathrm{i}}{2\mathcal{F}(\mathrm{i}\omega_{\mathrm{m}})}\right]\mathrm{e}^{-\frac{\omega_{\mathrm{m}}}{v_f}(x-x')}. \tag{B.10}$$

The 'non-interacting' Green functions $G^{(0);a,b}_{\uparrow 1}(\mathrm{i}\omega_{\mathrm{m}}; x, x')$ for $x - x' > 0$ are given by:

$$G^{(0);a,b}_{\uparrow 1}(\mathrm{i}\omega_{\mathrm{m}}; x, x') = \int \mathrm{d}p\, \frac{\mathrm{e}^{\mathrm{i}p(x-x')}}{v_f p - \mathrm{i}\omega_{\mathrm{m}}} = \frac{2\pi\mathrm{i}}{v_f}\theta(\omega_{\mathrm{m}})\mathrm{e}^{-\frac{\omega_{\mathrm{m}}}{v_f}(x-x')}\delta^{a,b}. \tag{B.11}$$

From equation (B.11), we see that equations (B.9), (B.10) take the form

$$G^{\mathrm{I,I}}_{\uparrow 1}(\mathrm{i}\omega_{\mathrm{m}}; x, x') = G^{(0);\mathrm{I,I}}_{\uparrow 1}(\mathrm{i}\omega_{\mathrm{m}}; x, x')\left[1 - 2\pi\mathrm{i}\frac{\lambda'}{1 + 2\lambda'\mathcal{F}(\mathrm{i}\omega_{\mathrm{m}})}\right] \tag{B.12}$$

and

$$G^{\mathrm{I,I}}_{\uparrow 1}(\mathrm{i}\omega_{\mathrm{m}}; x, x') = G^{(0);\mathrm{I,I}}_{\uparrow 1}(\mathrm{i}\omega_{\mathrm{m}}; x, x')\left[2\pi\mathrm{i}\frac{\mathrm{i}\lambda'}{1 + 2\lambda'\mathcal{F}(\mathrm{i}\omega_{\mathrm{m}})}\right]. \tag{B.13}$$

From equations (B.12), (B.13), we derive the S matrix elements in section 4.

Appendix C. Action of H_{T} on the various states

In this appendix, we show in detail how h_{T} acts on the states arising from hybridization of the impurity spin with the spin of itinerant lead electrons. This is the mathematical support to the derivation of section 5, where we use the results of this appendix to derive leading corrections to the fixed-point Hamiltonian.

The triplet states are:

$$
\begin{aligned}
&|\mathrm{Tri}, A, 1, \{\Xi\}\rangle = |\uparrow, A, \{\Xi\}\rangle \otimes |\Uparrow\rangle; \qquad |\mathrm{Tri}, B, 1, \{\Xi\}\rangle = |\uparrow, B, \{\Xi\}\rangle \otimes |\Uparrow\rangle;\\
&|\mathrm{Tri}, A, -1, \{\Xi\}\rangle = |\downarrow, A, \{\Xi\}\rangle \otimes |\Downarrow\rangle; \qquad |\mathrm{Tri}, B, -1, \{\Xi\}\rangle = |\downarrow, B, \{\Xi\}\rangle \otimes |\Downarrow\rangle;\\
&|\mathrm{Tri}, A, 0, \{\Xi\}\rangle = \frac{1}{\sqrt{2}}[|\uparrow, A, \{\Xi\}\rangle \otimes |\Downarrow\rangle + |\downarrow, A, \{\Xi\}\rangle \otimes |\Uparrow\rangle];\\
&|\mathrm{Tri}, B, 0, \{\Xi\}\rangle = \frac{1}{\sqrt{2}}[|\uparrow, B, \{\Xi\}\rangle \otimes |\Downarrow\rangle + |\downarrow, B, \{\Xi\}\rangle \otimes |\Uparrow\rangle].
\end{aligned}
\tag{C.1}
$$

Let us introduce the lattice operators b_X given by:

$$
b_X(x) \equiv \sqrt{\frac{2\pi\eta}{L}} :\mathrm{e}^{-\mathrm{i}\phi_X(na)}:; \qquad X = \mathrm{sp}, \mathrm{sf}. \tag{C.2}
$$

To start the derivation, let us rewrite H_{Red} in a lattice form, by using the operators b_{sp}, b_{fl}. We get the reduced lattice kinetic energy operator $H_{\mathrm{T,Red}}$, given by:

$$
\begin{aligned}
H_{\mathrm{T,Red}} = \sum_{x, X=\mathrm{sp,sf}} \{ & b_X^\dagger(x) b_X(x) - t[b_X^\dagger(x)(b_X(x+a) + b_X(x-a))\\
& + (b_X^\dagger(x+a) + b_X^\dagger(x-a)) b_X(x)]\}.
\end{aligned}
\tag{C.3}
$$

From the operator in equation (C.3), we may single out the term that acts on the Fock spaces of the states formed by hybridization between the spin of the localized impurity at the origin, and the spin of conduction electrons at $x = \pm a$. Such a term is given by:

$$
h_{\mathrm{T}} = -t \sum_{X=\mathrm{sp,sf}} [b_X^\dagger(0)(b_X(a) + b_X(-a)) + (b_X^\dagger(a) + b_X^\dagger(-a)) b_X(0)].
$$

The action of h_{T} on the singlets is given by:

$$
\begin{aligned}
h_{\mathrm{T}}|\mathrm{Sin}, A\rangle = {} & \frac{t}{\sqrt{2}}\{[b_{\mathrm{sp}}(a) + b_{\mathrm{sp}}(-a)]|\mathrm{Tri}, B, 1\rangle - [b_{\mathrm{sp}}^\dagger(a) + b_{\mathrm{sp}}^\dagger(-a)]|\mathrm{Tri}, B, -1\rangle\}\\
& - \frac{t}{2}[b_{\mathrm{sf}}(a) + b_{\mathrm{sf}}(-a) + b_{\mathrm{sf}}^\dagger(a) + b_{\mathrm{sf}}^\dagger(-a)]|\mathrm{Sin}, B\rangle\\
& + \frac{t}{2}[b_{\mathrm{sf}}(a) + b_{\mathrm{sf}}(-a) - b_{\mathrm{sf}}^\dagger(a) - b_{\mathrm{sf}}^\dagger(-a)]|\mathrm{Tri}, B, 0\rangle
\end{aligned}
\tag{C.4}
$$

and by:

$$
\begin{aligned}
h_{\mathrm{T}}|\mathrm{Sin}, B\rangle = {} & \frac{t}{\sqrt{2}}\{[b_{\mathrm{sp}}(a) + b_{\mathrm{sp}}(-a)]|\mathrm{Tri}, A, 1\rangle - [b_{\mathrm{sp}}^\dagger(a) + b_{\mathrm{sp}}^\dagger(-a)]|\mathrm{Tri}, A, -1\rangle\}\\
& - \frac{t}{2}[b_{\mathrm{sf}}(a) + b_{\mathrm{sf}}(-a) + b_{\mathrm{sf}}^\dagger(a) + b_{\mathrm{sf}}^\dagger(-a)]|\mathrm{Sin}, A\rangle\\
& - \frac{t}{2}[b_{\mathrm{sf}}(a) + b_{\mathrm{sf}}(-a) - b_{\mathrm{sf}}^\dagger(a) - b_{\mathrm{sf}}^\dagger(-a)]|\mathrm{Tri}, A, 0\rangle.
\end{aligned}
\tag{C.5}
$$

When acting on the triplet states, instead, h_{T} provides the following results:

$$
\begin{aligned}
h_{\mathrm{T}}|\mathrm{Tri}, A, 1\rangle = {} & -t[b_{\mathrm{sf}}^\dagger(a) + b_{\mathrm{sf}}^\dagger(-a)]|\mathrm{Tri}, B, 1\rangle + \frac{t}{\sqrt{2}}[b_{\mathrm{sp}}^\dagger(a) + b_{\mathrm{sp}}^\dagger(-a)]|\mathrm{Sin}, B\rangle\\
& - \frac{t}{\sqrt{2}}[b_{\mathrm{sp}}^\dagger(a) + b_{\mathrm{sp}}^\dagger(-a)]|\mathrm{Tri}, B, 0\rangle
\end{aligned}
\tag{C.6}
$$

$$
\begin{aligned}
h_{\mathrm{T}}|\mathrm{Tri}, B, 1\rangle = {} & -t[b_{\mathrm{sf}}(a) + b_{\mathrm{sf}}(-a)]|\mathrm{Tri}, A, 1\rangle + \frac{t}{\sqrt{2}}[b_{\mathrm{sp}}^\dagger(a) + b_{\mathrm{sp}}^\dagger(-a)]|\mathrm{Sin}, A\rangle\\
& - \frac{t}{\sqrt{2}}[b_{\mathrm{sp}}^\dagger(a) + b_{\mathrm{sp}}^\dagger(-a)]|\mathrm{Tri}, A, 0\rangle
\end{aligned}
\tag{C.7}
$$

$$h_{\mathrm{T}}|\mathrm{Tri},A,-1\rangle = -t[b_{\mathrm{sf}}(a)+b_{\mathrm{sf}}(-a)]|\mathrm{Tri},B,-1\rangle - \frac{t}{\sqrt{2}}[b_{\mathrm{sp}}(a)+b_{\mathrm{sp}}(-a)]|\mathrm{Sin},B\rangle - \frac{t}{\sqrt{2}}[b_{\mathrm{sp}}(a)+b_{\mathrm{sp}}(-a)]|\mathrm{Tri},B,0\rangle \tag{C.8}$$

$$h_{\mathrm{T}}|\mathrm{Tri},B,-1\rangle = -t[b^{\dagger}_{\mathrm{sf}}(a)+b^{\dagger}_{\mathrm{sf}}(-a)]|\mathrm{Tri},A,-1\rangle - \frac{t}{\sqrt{2}}[b_{\mathrm{sp}}(a)+b_{\mathrm{sp}}(-a)]|\mathrm{Sin},A\rangle - \frac{t}{\sqrt{2}}[b_{\mathrm{sp}}(a)+b_{\mathrm{sp}}(-a)]|\mathrm{Tri},A,0\rangle \tag{C.9}$$

$$\begin{aligned} h_{\mathrm{T}}|\mathrm{Tri},A,0\rangle = &-\frac{t}{\sqrt{2}}\{[b_{\mathrm{sp}}(a)+b_{\mathrm{sp}}(-a)]|\mathrm{Tri},B,1\rangle + [b^{\dagger}_{\mathrm{sp}}(a)+b^{\dagger}_{\mathrm{sp}}(-a)]|\mathrm{Tri},B,-1\rangle\} \\ &-\frac{t}{2}\{[b_{\mathrm{sf}}(a)+b_{\mathrm{sf}}(-a)+b^{\dagger}_{\mathrm{sf}}(a)+b^{\dagger}_{\mathrm{sf}}(-a)]\}|\mathrm{Tri},B,0\rangle \\ &-[b_{\mathrm{sf}}(a)+b_{\mathrm{sf}}(-a)-b^{\dagger}_{\mathrm{sf}}(a)-b^{\dagger}_{\mathrm{sf}}(-a)]|\mathrm{Sin},B\rangle\} \end{aligned} \tag{C.10}$$

$$\begin{aligned} h_{\mathrm{T}}|\mathrm{Tri},B,0\rangle = &-\frac{t}{\sqrt{2}}\{[b_{\mathrm{sp}}(a)+b_{\mathrm{sp}}(-a)]|\mathrm{Tri},A,1\rangle + [b^{\dagger}_{\mathrm{sp}}(a)+b^{\dagger}_{\mathrm{sp}}(-a)]|\mathrm{Tri},A,-1\rangle\} \\ &-\frac{t}{2}\{[b_{\mathrm{sf}}(a)+b_{\mathrm{sf}}(-a)+b^{\dagger}_{\mathrm{sf}}(a)+b^{\dagger}_{\mathrm{sf}}(-a)]\}|\mathrm{Tri},A,0\rangle \\ &+[b_{\mathrm{sf}}(a)+b_{\mathrm{sf}}(-a)-b^{\dagger}_{\mathrm{sf}}(a)-b^{\dagger}_{\mathrm{sf}}(-a)]|\mathrm{Sin},A\rangle\}. \end{aligned} \tag{C.11}$$

The equations listed above are all we need in order to work out subleading corrections to the fixed point Hamiltonian.

We apply the Schrieffer–Wolff transformation introduced in equation (38) by including just the hopping term between sites nearest neighbours of the impurity. The effective perturbative potential is:

$$V_{\mathrm{Eff}} \approx \mathbf{P}_0\left\{(h_{\mathrm{T}}+H_{\mathrm{K}}) + \frac{1}{E_{\mathrm{S}}-E_{\mathrm{T}}}[h_{\mathrm{T}}[\mathbf{1}-\mathbf{P}_0]h_{\mathrm{T}}] + \left(\frac{1}{E_{\mathrm{S}}-E_{\mathrm{T}}}\right)^2[h_{\mathrm{T}}[\mathbf{1}-\mathbf{P}_0]h_{\mathrm{T}}[\mathbf{1}-\mathbf{P}_0]h_{\mathrm{T}}]\right\}\mathbf{P}_0. \tag{C.12}$$

The first term on the rhs of equation (C.12), can be expressed in terms of the operators $\mathcal{Q}_0$ and $\mathcal{Q}_{\pm a}$, leading to the equation (39).

The $\mathcal{O}(t^2/J)$ of equation (C.12) provides the following matrix elements:

$$M^2_{AB} = M^2_{BA} = 0; \qquad M^2_{AA} = M^2_{BB} = \frac{2t^2}{E-\frac{7}{4}J} \approx -\frac{t^2}{2J}. \tag{C.13}$$

Therefore, on $|\mathrm{Sin},\pm,\{\Xi\}\rangle$, second-order (in t) dynamics just yields an overall trivial shift of each energy eigenvalue by a constant amount.

Non-trivial, effects, instead, arise from third-order corrections. Indeed, while we have once more:

$$M^3_{AA} = M^3_{BB} = 0, \tag{C.14}$$

on the other hand, we obtain:

$$\begin{aligned} (4J)^2 M^3_{AB} &= \sum_{XX'}\langle \mathrm{Sin},A,\{\Xi\}|h_{\mathrm{T}}|E_X\rangle\langle E_X|h_{\mathrm{T}}|E_{X'}\rangle\langle E_{X'}|h_{\mathrm{T}}|\mathrm{Sin},B\rangle \\ &= -\frac{3t^3}{4}(b_{\mathrm{sf}}(a)+b_{\mathrm{sf}}(-a)+b^{\dagger}_{\mathrm{sf}}(a)+b^{\dagger}_{\mathrm{sf}}(-a)) - \frac{t^3}{4}[(b_{\mathrm{sp}}(a)+b_{\mathrm{sp}}(-a)), \\ &\quad (b^{\dagger}_{\mathrm{sp}}(a)+b^{\dagger}_{\mathrm{sp}}(-a))](b_{\mathrm{sf}}(a)+b_{\mathrm{sf}}(-a)-b^{\dagger}_{\mathrm{sf}}(a)-b^{\dagger}_{\mathrm{sf}}(-a)), \end{aligned} \tag{C.15}$$

where $|E_X\rangle$ is a generic high-energy triplet.

From equation (C.15), we see that M^3_{AB} contains a contribution proportional to the term we found to $\mathcal{O}(t)$. Therefore, it may be accounted for by means of a slight renormalization of λ', that is $\mathcal{O}(t^3/J^2)$ and is absolutely irrelevant. Since this effect is trivial, we will not consider it here. The non-trivial part of the correction operator can be derived by recalling the basic bosonization rules listed in appendix A. In particular, we obtain the following expression for the commutator in equation (C.15):

$$[(b^\dagger_{\rm sp}(a)+b^\dagger_{\rm sp}(-a)),(b_{\rm sp}(a)+b_{\rm sp}(-a))]=\frac{1}{\pi}\frac{{\rm d}\Psi_{\rm sp}(0)}{{\rm d}x}. \tag{C.16}$$

Therefore, taking the limit $a\to 0$ in the regular part of the result in equation (C.15), we get the result:

$$M^3_{AB}=M_3=\frac{t^3}{\pi J^2}\sin[\Psi_{\rm sf}(0)]\frac{{\rm d}\Psi_{\rm sp}(0)}{{\rm d}x} \tag{C.17}$$

plus the irrelevant terms discussed before.

Appendix D. Calculation of leading finite-frequency corrections to the S-matrix

In this appendix, we will show in detail how to calculate leading finite-frequency corrections to the S-matrix. To do so, first of all, let us recall what the relevant correlators we need are. We may calculate them according to the basic bosonization rules of appendix A (and to the fact that all the involved fields are chiral). We obtain:

$$\langle\mathcal{T}_\tau[:{\rm e}^{-\frac{\rm i}{2}\Psi(x,\tau)}:\,:{\rm e}^{\frac{\rm i}{2}\Psi(x',\tau')}:]\rangle=\frac{1}{\left[{\rm e}^{\frac{2\pi{\rm i}}{L}(x+{\rm i}v_f\tau)}-{\rm e}^{\frac{2\pi{\rm i}}{L}(x'+{\rm i}v_f\tau')}\right]^{\frac14}} \tag{D.1}$$

(this will provide us with the charge–charge and the flavour–flavour part of the relevant correlator).

Moreover, we get:

$$\left\langle\mathcal{T}_\tau\left[:{\rm e}^{-\frac{\rm i}{2}\Psi_{\rm sp}(x,\tau)}:\frac{\partial\Psi_{\rm sp}(0,\tau_1)}{\partial x}:{\rm e}^{\frac{\rm i}{2}\Psi_{\rm sp}(x',\tau')}:\right]\right\rangle$$
$$=-\frac{\pi}{L}\frac{{\rm e}^{\frac{2\pi v_f}{L}\tau_1}[{\rm e}^{\frac{2\pi{\rm i}}{L}(x+{\rm i}v_f\tau)}-{\rm e}^{\frac{2\pi{\rm i}}{L}(x'+{\rm i}v_f\tau')}]^{\frac34}}{[{\rm e}^{\frac{-2\pi v_f}{L}\tau_1}-{\rm e}^{\frac{2\pi{\rm i}}{L}(x+{\rm i}v_f\tau)}][{\rm e}^{\frac{-2\pi v_f}{L}\tau_1}-{\rm e}^{\frac{2\pi{\rm i}}{L}(x'+{\rm i}v_f\tau')}]}. \tag{D.2}$$

Finally, we obtain:

$$\langle\mathcal{T}_\tau[:{\rm e}^{-\frac{\rm i}{2}\Psi_{\rm sf}(x,\tau)}:\,:{\rm e}^{{\rm i}\Psi_{\rm sf}(0,\tau_1)}:\,:{\rm e}^{-\frac{\rm i}{2}\Psi_{\rm sf}(x',\tau')}:]\rangle=\langle\mathcal{T}_\tau[:{\rm e}^{\frac{\rm i}{2}\Psi_{\rm sf}(x,\tau)}:\,:{\rm e}^{-{\rm i}\Psi_{\rm sf}(0,\tau_1)}:\,:{\rm e}^{\frac{\rm i}{2}\Psi_{\rm sf}(x',\tau')}:]\rangle$$
$$=\frac{[{\rm e}^{\frac{2\pi{\rm i}}{L}(x+{\rm i}v_f\tau)}-{\rm e}^{\frac{2\pi{\rm i}}{L}(x'+{\rm i}v_f\tau')}]^{\frac14}}{[{\rm e}^{\frac{-2\pi v_f}{L}\tau_1}-{\rm e}^{\frac{2\pi{\rm i}}{L}(x+{\rm i}v_f\tau)}]^{\frac12}[{\rm e}^{-\frac{2\pi v_f}{L}\tau_1}-{\rm e}^{\frac{2\pi{\rm i}}{L}(x'+{\rm i}v_f\tau')}]^{\frac12}}. \tag{D.3}$$

By putting together all the correlators in equations (D.1)–(D.3), we obtain the integral in equation (49). To calculate the integral, we use as an auxiliary variable $\xi=\exp[-\frac{2\pi}{L}v_f\tau]$. Therefore, after all the substitutions and the variable replacements have been made, the integral reads:

$$\frac{{\rm i}t^3}{2\pi v_f J^2}\left(\frac{2\pi}{L}\right)^{\frac32}\int_0^1{\rm d}\xi\,\frac{[{\rm e}^{\frac{2\pi{\rm i}}{L}(x+{\rm i}v_f\tau)}-{\rm e}^{\frac{2\pi{\rm i}}{L}(x'+{\rm i}v_f\tau')}]^{\frac12}}{[\xi-{\rm e}^{\frac{2\pi{\rm i}}{L}(x+{\rm i}v_f\tau)}]^{\frac32}[\xi-{\rm e}^{\frac{2\pi{\rm i}}{L}(x'+{\rm i}v_f\tau')}]^{\frac32}}$$
$$=\frac{{\rm i}t^3}{2\pi v_f J^2}\frac{(2\pi/L)^{\frac32}}{[{\rm e}^{\frac{2\pi{\rm i}}{L}(x+{\rm i}v_f\tau)}-{\rm e}^{\frac{2\pi{\rm i}}{L}(x'+{\rm i}v_f\tau')}]^{\frac32}}\left\{\frac{[{\rm e}^{\frac{2\pi{\rm i}}{L}(x+{\rm i}v_f\tau)}+{\rm e}^{\frac{2\pi{\rm i}}{L}(x'+{\rm i}v_f\tau')}]}{\sqrt{{\rm e}^{\frac{2\pi{\rm i}}{L}(x+{\rm i}v_f\tau)}{\rm e}^{\frac{2\pi{\rm i}}{L}(x'+{\rm i}v_f\tau')}}}\right.$$
$$\left.-\frac{[{\rm e}^{\frac{2\pi{\rm i}}{L}(x+{\rm i}v_f\tau)}+{\rm e}^{\frac{2\pi{\rm i}}{L}(x'+{\rm i}v_f\tau')}]-2}{\sqrt{({\rm e}^{\frac{2\pi{\rm i}}{L}(x+{\rm i}v_f\tau)}-1)({\rm e}^{\frac{2\pi{\rm i}}{L}(x'+{\rm i}v_f\tau')}-1)}}\right\} \tag{D.4}$$

(notice the extra prefactor of $(2\pi/L)^{\frac{3}{2}}$, which we have introduced in order to make the bosonization rules of appendix A consistent with the normalization for the Green functions introduced in appendix B).

In section 6 we point out that the integral in equation (D.4) is computed in the limit of very large L, β. Such a limit yields the ultimate approximate formula:

$$\frac{\mathrm{i}t^3}{2\pi v_f J^2}\left(\frac{1}{\mathrm{i}}\right)^{\frac{3}{2}} \frac{1}{[x-x'+\mathrm{i}v_f\tau]^{\frac{3}{2}}}. \tag{D.5}$$

When going back to (Matsubara) frequency space, we have to calculate:

$$\frac{\mathrm{i}t^3}{2\pi v_f J^2}\left(\frac{1}{\mathrm{i}}\right)^{\frac{3}{2}} \int_{-\infty}^{\infty} \mathrm{d}\tau \, \frac{\mathrm{e}^{\mathrm{i}\omega_{\mathrm{m}}\tau}}{[x-x'+\mathrm{i}v_f\tau]^{\frac{3}{2}}}. \tag{D.6}$$

The integral in equation (D.6) is calculated as follows:

$$\begin{aligned}
&\frac{\mathrm{i}t^3}{2\pi v_f J^2}\left(\frac{1}{\mathrm{i}}\right)^{\frac{3}{2}} \int_{-\infty}^{\infty} \mathrm{d}\tau \, \frac{\mathrm{e}^{\mathrm{i}\omega_{\mathrm{m}}\tau}}{[x-x'+\mathrm{i}v_f\tau]^{\frac{3}{2}}} \\
&\quad = \frac{-\mathrm{i}t^3}{\pi v_f J^2}\left(\frac{1}{\mathrm{i}}\right)^{\frac{3}{2}} \frac{\partial}{\partial x} \int_{-\infty}^{\infty} \frac{\mathrm{d}s}{\sqrt{\pi}} \mathrm{e}^{-s^2(x-x')} 2\pi \int_{-\infty}^{\infty} \mathrm{d}\tau \, \mathrm{e}^{\mathrm{i}\tau(\omega_{\mathrm{m}}-s^2 v_f)} \\
&\quad = -\frac{\mathrm{i}t^3}{J^2}\sqrt{\frac{\omega_{\mathrm{m}}}{\pi v_f}} (\mathrm{i}v_f)^{-\frac{3}{2}} \theta(\omega_{\mathrm{m}}) \mathrm{e}^{-\frac{\omega_{\mathrm{m}}}{v_f}(x-x')}
\end{aligned} \tag{D.7}$$

with $x - x' > 0$.

When rotating back to real times/frequencies, the result in equation (D.7) reads:

$$-\frac{t^3}{J^2 v_f^{\frac{3}{2}}}\sqrt{\frac{|\omega|}{\pi v_f}} \mathrm{e}^{\mathrm{i}\frac{\omega}{v_f}(x-x')}. \tag{D.8}$$

By going back to real frequency, this provides the finite-frequency correction to the **S**-matrix that we have used in section 6 to derive the conductance.

References

[1] Kondo J 1966 *J. Appl. Phys.* **37** 1177
Tsvelick A M and Wiegmann P B 1983 *Adv. Phys.* **32** 453

[2] Glazman L I and Raikh M E 1988 *Pis. Zh. Eksp. Teor. Fiz.* **47** 378
Glazman L I and Raikh M E 1988 *JETP Lett.* **47** 452 (Engl. Transl.)
Ng T K and Lee P A 1988 *Phys. Rev. Lett.* **61** 1768
Meir Y, Wingreen N S and Lee P A 1993 *Phys. Rev. Lett.* **70** 2601

[3] Goldhaber-Gordon D, Shtrikman H, Mahalu D, Abusch-Magder D, Meirav U and Kastner M A 1998 *Nature* **391** 156
Cronenwett S M, Oosterkamp T H and Kouwenhoven L P 1998 *Science* **281** 540

[4] van der Wiel W G, De Franceschi S, Fujisawa T, Elzerman J M, Tarucha S and Kouwenhoven L P 2000 *Science* **289** 2105

[5] Noziéres P and Blandin A 1980 *J. Physique* **41** 193

[6] Vladàr K and Zawadowski A 1983 *Phys. Rev.* B **28** 1564–81
Vladàr K and Zawadowski A 1983 *Phys. Rev.* B **28** 1582–95
Vladàr K and Zawadowski A 1983 *Phys. Rev.* B **28** 1596–612

[7] Noziéres P 1974 *J. Low Temp. Phys.* **17** 31

[8] Eto M and Nazarov Y 2000 *Phys. Rev. Lett.* **85** 1306

[9] Giuliano D and Tagliacozzo A 2000 *Phys. Rev. Lett.* **84** 4677
Giuliano D, Jouault B and Tagliacozzo A 2001 *Phys. Rev.* B **63** 125318

[10] Pustilnik M, Glazman L I, Cobden D H and Kouwenhoven L P 2001 *Lecture Notes in Physics* vol 579 (Heidelberg: Springer) p 3

Pustilnik M and Glazman L I 2001 *Phys. Rev. Lett.* **85** 2993
Pustilnik M and Glazman L I 2001 *Phys. Rev.* B **64** 045328
[11] Affleck I and Ludwig A W W 1993 *Phys. Rev.* B **48** 7297
Affleck I and Ludwig A W W 1991 *Nucl. Phys.* B **352** 849
Affleck I and Ludwig A W W 1991 *Nucl. Phys.* B **360** 641
Affleck I and Ludwig A W W 1991 *Phys. Rev. Lett.* **67** 161
[12] Borda L, Zawadowski A and Zaràn G 2003 *Phys. Rev.* B **68** 045114
[13] Zawadowski A 1980 *Phys. Rev. Lett.* **45** 211
[14] Zawadowski A and Zaràn G 1994 *Phys. Rev. Lett.* **72** 542
Zawadowski A and Zaràn G 1994 *Phys. Rev.* B **50** 932 (*Preprint* cond-mat/0009283)
Aleiner I L, Altshuler B L, Galperin Y M and Shutenko T A 2001 *Phys. Rev. Lett.* **86** 2629
[15] Ralph D C, Ludwig A W W, von Delft J and Buhrman R A 1994 *Phys. Rev. Lett.* **72** 1064
Upadhyay S K, Louie R N and Buhrman R A 1997 *Phys. Rev.* B **56** 12033
[16] Giuliano D, Jouault B and Tagliacozzo A 2002 *Europhys. Lett.* **58** 401
[17] Oreg Y and Goldhaber-Gordon D 2003 *Phys. Rev. Lett.* **90** 136602
Florens S and Rosch A 2004 *Phys. Rev. Lett.* **92** 216601
[18] Pustilnik M, Borda L, Glazman L I and von Delft J 2004 *Phys. Rev.* B **69** 115316
[19] See for instance, Morandi G *et al* (ed) 2000 *Field Theories for Low-Dimensional Condensed Matter Systems* (*Springer Series in Solid-State Sciences*) (Berlin: Springer)
[20] Andrei N and Destri C 1984 *Phys. Rev. Lett.* **52** 364
Wiegmann P B and Tsvelick A M 1985 *Z. Phys.* B **54** 201
Tsvelick A M 1985 *J. Phys. C: Solid State Phys.* **18** 159
Costi T A and Zaránd G 1999 *Phys. Rev.* B **59** 12398
[21] Wilson K G 1975 *Rev. Mod. Phys.* **47** 773
Krishnamurthy H R, Wilkins J W and Wilson K G 1980 *Phys. Rev.* B **21** 1003
[22] Frota H O and Oliveira L N 1986 *Phys. Rev.* B **33** 7871(R)
Muramatsu A and Guinea F 1986 *Phys. Rev. Lett.* **57** 2337
[23] Costi T A 2001 *Phys. Rev.* B **64** 24130(R)
Costi T A 2000 *Phys. Rev. Lett.* **85** 1504
[24] Sakai O and Shimizu Y 1992 *J. Phys. Soc. Japan* **61** 2333
Sakai O, Suzuki S and Shimizu Y 1995 *J. Physica* B **206/207** 141
Izumida W, Sakai O and Shimizu Y 1997 *J. Phys. Soc. Japan* **66** 717
[25] Emery V J and Kivelson S 1992 *Phys. Rev.* B **46** 10812
Emery V J and Kivelson S 1993 *Phys. Rev. Lett.* **71** 3701
[26] von Delft J, Zaránd G and Fabrizio M 1998 *Phys. Rev. Lett.* **81** 196
[27] Coleman P, Ioffe L and Tsvelick A M 1995 *Phys. Rev.* B **52** 6611
[28] Kroha J, Wölfle P and Costi T A 1997 *Phys. Rev. Lett.* **79** 261
[29] Anderson P W 1970 *J. Phys. C: Solid State Phys.* **3** 2436
Fabrizio M, Gogolin A O and Noziéres Ph 1995 *Phys. Rev.* B **51** 16088
[30] Meir Y and Wingreen N S 1994 *Phys. Rev.* B **49** 11040
[31] Hettler M H, Kroha J and Hershfield S 1998 *Phys. Rev.* B **58** 5649
Costi T A, Kroha J and Wölfle P 1996 *Phys. Rev.* B **53** 1850
Haule K, Kirchner S, Kroha J and Wölfle P 2001 *Phys. Rev.* B **64** 155111
[32] Koenig J, Schmidt J, Schoeller H and Schon G 1996 *Phys. Rev.* B **54** 16820
Koenig J, Schmidt J, Schoeller H and Schon G 1996 *Czech. J. Phys.* **46** 2399
[33] Schoeller H and Schon G 1994 *Phys. Rev.* B **50** 18436
Koenig J and Schoeller H 1998 *Phys. Rev. Lett.* **81** 3511
Schoeller H 2000 *Lecture Notes in Physics* vol 544 (Heidelberg: Springer) p 137
Schoeller H and Koenig J 2000 *Phys. Rev. Lett.* **84** 3686
[34] Maldacena J M and Ludwig A M M 1997 *Nucl. Phys.* B **506** 565
[35] Tagliacozzo A and Tosatti E 1988 *Phys. Scr.* **38** 301
[36] Konik R M, Saleur H and Ludwig A 2002 *Phys. Rev.* B **66** 125304
Konik R M, Saleur H and Ludwig A 2001 *Phys. Rev. Lett.* **87** 236801
[37] Costi T A, Hewson A C and Zlatic V 1994 *J. Phys.: Condens. Matter* **6** 2519
Costi T A and Hewson A C 1992 *Phil. Mag.* B **65** 1165
[38] Affleck I, Ludwig A W W, Pang H B and Cox D L 1992 *Phys. Rev.* B **45** 7918
Costi T A 1998 *Phys. Rev. Lett.* **80** 1038